MINISTRY OF SUPPLY

AERONAUTICAL RESEARCH COUNCIL
REPORTS AND MEMORANDA

Model Tests on an Air Interchange System for Removing Engine Exhaust Products from a Wind Tunnel

By

K. W. NEWBY, D.Ae., E. G. BARNES, A.M.I.Mech.E.
and D. W. BOTTLE, B.Sc.

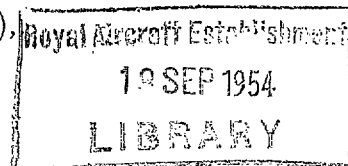LONDON : HER MAJESTY'S STATIONERY OFFICE

1954

NINE SHILLINGS NET

Model Tests on an Air Interchange System for Removing Engine Exhaust Products from a Wind Tunnel

By

K. W. Newby, D.Ae., E. G. Barnes, A.M.I.Mech.E.
and D. W. Bottle, B.Sc.

Summary.—Model tests have been made to investigate the functioning of an air interchange system for removing from a return-circuit wind tunnel a high proportion of the exhaust products from propulsive units under test.

The tests were planned to assist the design of an engine altitude tunnel. With changing circumstances the priority of this tunnel has been reduced, but the tests were continued to give general information on the extraction of engine exhaust products from this type of wind tunnel.

The tests were made on a partial model of a tunnel, which had an air interchange exhaust collector designed to remove 15 per cent of the tunnel mass flow. This was installed on the tunnel axis at the downstream end of the working section. Tests were also made on 10 per cent and 5 per cent collector entries designed to be interchangeable with the 15 per cent entry. The main results obtained were as follows:—

1. The flow in the working-section was satisfactory, and was not affected by substituting the 5 per cent or 10 per cent collector for the 15 per cent collector, nor was it affected by changes made to the interchange ratio with a given collector.

2. The flow of the main tunnel air round the collectors and in the annular diffuser downstream of the collectors was satisfactory. The losses at the collectors were of the order expected, but were appreciable, and would increase the fan power required to drive a normal tunnel by some 20 to 30 per cent. The wake from the collector duct affected the flow distribution in the return circuit, but this could be corrected by screens at the maximum section of the tunnel.

3. The losses in the interchange air with the 15 per cent collector and duct system were satisfactorily small. These losses were larger for the smaller collectors, but could be reduced.

4. A model in the tunnel working-section had no serious effects on the main and interchange flow.

5. With the 15 per cent interchange system as designed, lower interchange ratios can be obtained by reducing the suction at the collector or by installing smaller interchangeable collectors. The first method is more economical as regards exhausting compressor power, the second is preferable if it is more important to keep the tunnel fan power down.

6. The design of the 16:1 area ratio contraction cone used was economic and satisfactory.

The tests have confirmed that the interchange system tested was generally very satisfactory for the specified requirements, and that in the interests of power economy, the interchange ratio should be reduced as far as possible.

In other tunnels with less exacting requirements the collector duct would of course be placed in a region where the wind speed was low, in order to reduce the losses and hence the fan power.

---

1. *Introduction.*—In 1945 tests were proposed to investigate on a model scale the air interchange system of a 25-ft diameter wind tunnel, planned for the testing of engine installations under altitude conditions, up to high subsonic Mach numbers. With changing circumstances the need for an engine altitude-tunnel to this specification, and the facilities available for its construction, have diminished.

Basic information on methods of removing undesirable exhaust products from return-circuit wind tunnels is still needed however, particularly in connection with any future tunnel work on ram jets. A shortened programme of tests, therefore, has been made on a 1/30th scale partial model of the altitude engine tunnel, up to choking speeds.

From the requirements of the air interchange system of an engine altitude-tunnel it was concluded that the interchange ratio

$$\mu = \frac{\text{Interchange mass flow}}{\text{Tunnel mass flow}}$$

must be of the order of 0·15 in order that the selected tunnel cooling system shall function properly, and to ensure that a very high proportion of the exhaust products of most of the propulsive systems likely to be tested, shall be removed from the tunnel.

The collector duct then had to be designed so as to:—

(a) interfere as little as possible with the working-section flow,

(b) give efficient and uniform diffusion of the main tunnel flow up to the first corner of the tunnel,

(c) give efficient diffusion of the interchange air out of the tunnel, to the exhausting compressors.

The design selected and tested is shown in Figs. 1 and 2.

In any tunnel where an interchange system is necessary, it is desirable to keep the interchange mass flow ratio μ, as small as possible, consistent with satisfactory functioning, in order to avoid unnecessarily large disturbances in the main tunnel flow.

A low value of μ is even more important in sub-atmospheric and pressurised tunnels, since the capacity of compressors and other auxiliaries needed to operate the interchange system for such tunnels, is large, and is proportional to μ. Also for high-speed tests, the interchange air has to be dried to avoid spurious compressibility effects, and the size of the drying plant will again be proportional to μ.

It was, therefore, decided to test, in addition to the 15 per cent collector, two alternative collector entries, extracting 10 per cent and 5 per cent of the tunnel mass flow respectively, the aim being to develop collectors which could be fitted with the minimum of modification to the 15 per cent system. These smaller collectors could then be used if the collection of exhaust products proved easier than was expected, or if some tunnel contamination could be permitted*.

The other side of the interchange system, the introduction of clean air into the tunnel, is not expected to present serious difficulties and has not been investigated in the present tests.

---

* To meet the specification of the engine altitude-tunnel with the selected cooling system it was necessary to remove a very high proportion of exhaust products in order that water from the exhausts should not build up as ice in the tunnel. This criterion may be less exacting in other types of tunnel for engine or ram jet tests. If some build-up of exhaust products in the tunnel is permissible then it may be economical to move the air interchange collector further downstream from the working-section.

2. *Description of Apparatus.*—2.1. *The Test Rig.*—The layout of the partial model of the tunnel is shown in Fig. 1. The model represented the contraction cone, working-section and first diffuser of a return-circuit wind tunnel. The collector duct to extract exhaust products from the tunnel air stream was mounted in the first diffuser close to the working-section. It was proposed to run this partial model tunnel as a straight through or National Physical Laboratory type tunnel with atmospheric entry using the exhausting compressors of the Royal Aircraft Establishment high-altitude plant. Fig. 1 also shows the entry flare and the ducting from the partial model to the exhausting compressor main.

To avoid the need for a separate exhausting compressor for the interchange air, the interchange air duct was returned to the main tunnel duct just before its connection to the exhauster main. Control of the air interchange ratio was obtained by inserting gauze resistances downstream of the model tunnel, and by operation of the butterfly valve in the air interchange circuit (*see* Fig. 1).

The capacity of the exhausting compressors limited the size of working-section, for which it would be convenient to attain choking speed with atmospheric entry conditions, to 10 in. diameter. This size of model could be fitted conveniently into the building.

2.2. *Geometry of Tunnel.*—2.2.1. *General arrangement.*—A general arrangement of the model is shown in Fig. 1, and its main dimensions are given in Tables 1 and 2. A more detailed section of the air interchange collector and the surrounding tunnel shell is shown in Fig. 2. The tunnel was of circular section throughout, except for the interchange aerofoil ducts, and the associated ducting shown in section X—X of Fig. 2.

The entry flare guided the incoming atmospheric air into a short settling chamber 8 in. long and 40 in diameter which represented the maximum section of the full-scale tunnel. The contraction cone had an area ratio of 16:1. Its shape was chosen empirically and the lines are given in Table 1.

The working-section was given a uniform expansion along the whole of its length, to allow for the boundary-layer growth, the rate of expansion being based on theoretical calculations by Emerson and Young[1].

The main shell of the first diffuser (Fig. 1) had a total geometrical cone angle of 7 deg, the actual rate of diffusion being reduced to that of an equivalent 5 deg cone angle diffuser, by the installation of the air interchange collector tube, which was concentric with the main shell.

Between the end of the first diffuser and the beginning of the second, the tunnel formed an annular duct of constant cross-sectional area, bounded by the main shell, and the interchange collector fairing. The second diffuser was of conventional form, with a total cone angle of 5 deg.

2.2.2. *Alternative collector entries.*—The geometry of the three interchange air collector entries is shown in Fig. 3. The alternative 5 per cent and 10 per cent entries were designed to be easily interchangeable with the basic 15 per cent entry, and also the length of the interchangeable parts was kept down so that they could be inserted into or removed from the tunnel at the working-section. These were considered to be important requirements for the full-scale tunnel.

The shape of the upstream end of the smaller collectors gave a constant cross-sectional area for the main tunnel flow and then faired into the 15 per cent collector tube. This geometry was expected to give reasonably good flow for the main tunnel air without any danger of choking the tunnel at high speeds. With the smaller collectors the interchange air was expected to suffer some entry loss, and had this proved serious, it was intended to fit liners inside the entry to round off the sharp edge at entry and give better internal diffusion.

2.3. *Construction.*—Timber was used in the construction of the main tunnel shell, from the entry flare to the end of the second diffuser. The air interchange collector tube, and the remainder of the tunnel circuit were of metal construction.

2.4. *Instrumentation.*—For the purpose of controlling the speed of the air in the working-section, two hole-in-side static pressure points were provided in the contraction cone, one at the maximum section and one just upstream of the working-section, while the interchange air mass flow was measured using a standard nozzle[2] shown in Fig. 1.

Wall static pressure tubes were fitted in the top and bottom walls along the whole length of the partial model, and also in the interchange aerofoil ducts, in the plane of the pitot traverses Fig. 2. Wall static tubes were also installed in the inner and outer walls of the 15 per cent collector entry just downstream of its leading edge as shown in Fig. 3. From these readings a rough indication of interchange ratio could be obtained.

Provision was made for the installation of static pressure or pitot traverses in the tunnel entry and working-section, for the purpose of calibration, (*see* Appendix I) and to determine the effect of variation of the interchange ratio on the velocity distribution across the working-section.

The pitot and static tubes used in the working-section were made from 1-mm outside diameter hypodermic tubing, mounted on the leading edge of a $\frac{1}{2}$-in. chord, 18·75 per cent thickness/chord ratio aerofoil section strut spanning the tunnel. This small size was required so as to avoid choking the tunnel at high Mach numbers.

Pitot combs were fitted on the leading edges of the air-interchange collector-tube supports (Fig. 2), in the first diffuser, and at the end of the second diffuser, the latter being of crucifix form, to obtain readings in both the horizontal and vertical planes.

Pitot traverse tubes were installed ahead of the interchange aerofoil ducts at the end of the first diffuser, and also in the aerofoil ducts themselves, three in each duct (Fig. 4).

3. *Tests.*—3.1. *Preliminary Tests.*—Preliminary tests were made, to calibrate the speed and mass flow of the tunnel, and to check the uniformity of flow in the entry and in the working section. Details of these calibration tests are given in Appendix I. The wall static pressure distribution down the contraction cone and working-section were also measured.

3.2. 15·6 *per cent Collector Entry.*—3.2.1. *Tests on the effect of variations of interchange ratio on the tunnel flow.*—Tests were made at Geometric Interchange Ratio* for $M_0 = 0·2$, $0·4$, $0·6$, $0·8$, $0·9$, measurements of all wall static pressures and pitot pressure traverses being taken.

The interchange ratio was then successively increased and decreased by about 10 per cent of the geometric interchange ratio, and the tests repeated.

To obtain a comparison between the working of the 15·6 per cent and the 10 per cent collector entries operating at the same interchange ratio, a test was made at $M_0 = 0·6$, with the 15·6 per cent collector installed, and the interchange ratio reduced to approximately 0·10.

3.2.2. *Tests on the influence of a wing spanning the working-section on the flow in the tunnel.*—A 3·5 in. chord, 10 per cent thickness/chord ratio, symmetrical aerofoil section wing was installed,

---

* The geometric interchange ratio μ_G is arbitrarily defined as follows:—

$$\mu_G = \frac{\text{Collector entry area}}{\text{Tunnel cross-sectional area in plane of collector entry}}$$

spanning the working-section. Tests were made in which all the wall static pressures and pitot pressure traverses, in the diffusers and interchange aerofoil ducts were measured, under the following conditions:—

(1) $M_0 = 0.20$ Aerofoil Incidence 0 deg

(2) $M_0 = 0.20$,, ,, 10 deg

(3) $M_0 = 0.50$,, ,, 0 deg

(4) $M_0 = 0.50$,, ,, 5 deg

The strength of the wing limited the incidence range at high speed. These tests were made at an interchange ratio of 0.156, i.e., geometrical interchange ratio.

3.3. 10.0 *per cent Collector Entry.*—Measurements of all wall static pressures, and pitot pressure traverses were made, for $M_0 = 0.2$, 0.6, and 0.8, at geometric interchange ratio, and for $M_0 = 0.2$, and 0.8, at an interchange ratio of 0.05, the latter tests giving a comparison with the 5 per cent collector entry.

Total head losses in the interchange air circuit were found to be too great, with the pressure balancing screens available, to attain more than geometric interchange ratio.

3.4. 5.0 *per cent Collector Entry.*—Total head losses in the interchange system were so large that the maximum interchange ratio and Mach number attainable were 0.045 and 0.75 respectively.

As in the previous tests, wall static pressures and pitot traverse pressures were measured, at the maximum attainable interchange ratio, for $M_0 = 0.2$, 0.6, and 0.75.

4. *Results.*—4.1. *Contraction Cone.*—At entry to the contraction cone the total head was uniform and equal to atmospheric pressure. The velocity distribution here, which is shown in Fig. 5, was fairly representative of conditions at the corresponding section of a return-circuit tunnel. Outside the boundary layer there was no measurable loss of head in the contraction cone, and both total head and static pressure distribution across the working-section were uniform within the limits of measurement (see Appendix I). Fig. 6 shows the static pressure variation along the walls of the contraction cone, from which it can be seen that there was neither a tendency for an adverse pressure gradient to build up on the concave walls at the low-speed section, nor for a suction peak to form on the convex walls towards the high-speed end. A comparison with the theoretical isentropic pressure distribution at $M_0 = 0.822$ shows extremely good agreement (Fig. 6).

The static pressure gradient at the end of the contraction cone is discussed in the next section.

4.2. *Working-Section.*—The velocity distribution across the working-section, 1.1 working-section diameters ahead of the collector entry was uniform over the speed range tested, to within 0.2 per cent of the velocity at the centre (Fig. 5) and was unaffected by small changes of interchange ratio.

As shown in Fig. 7, the variation of the interchange ratio, or the installation of different collector entries had no effect on the wall static pressure distribution down the working-section within the accuracy of measurement, i.e., $\frac{1}{2}$ per cent $\frac{1}{2}\rho_0 V_0^2$.

Typical curves showing the wall static pressure and corresponding Mach number down the working-section are shown in Figs. 8, 9, respectively. Fig. 10 shows the geometrical taper of the working-section, and also the effective working-section radii calculated from the observed wall static pressure assuming uniform isentropic flow.

5

It will be noted that the pressure, Mach number, and effective radius down the central half of the working-section length were all uniform up to a Mach number of $0 \cdot 82$. At $M = 0 \cdot 89$ the tunnel taper is slightly too small. At the beginning and end of the working-section there was a negative static pressure gradient whose magnitude increased with M. The pressure gradient at entry to the working-section could be accounted for by the rate of growth of the boundary layer in the almost parallel end of the contraction cone, and it would be safer to check the magnitude of this effect when designing contraction cones for high-speed tunnels. (*See* Appendix IV.)

At entry to the working-section the pressure gradient steepens slightly, probably due to a thickening of the boundary layer at the junction of the contraction cone and working-section. These pressure gradients at the entry to the working-section only assume importance at Mach numbers near 1 when minute changes of area effect appreciable pressure changes.

A reduction in wall pressure at the downstream end of the working-section would be expected due to the curvature of the flow at the entry to the first diffuser, and has been observed in a number of tunnels. For example in the Co-operative Tunnel at California Institute of Technology[3], the wall pressure shows a peak suction at the end of the working-section while the static pressure down the working-section axis starts to rise at the same cross-section.

4.3. *Diffusers (Main Flow).*—4.3.1. *Static pressure measurements.*—Fig. 11 shows the recovery of static pressure along the diffuser walls for the $15 \cdot 6$ per cent collector entry compared with the ideal recovery for isentropic frictionless flow. The static pressure efficiency η_p, which is quoted in Fig. 11, was almost constant, increasing from 83 per cent at $M = 0 \cdot 2$, to 85 per cent at $M = 0 \cdot 8$. Fig. 12 shows the effect of interchange ratio, Mach number, and collector entry size on the static pressure recovery. It will be noted that when the three collector entries are working at their geometrical interchange ratio their pressure efficiencies are practically the same. Operating the $15 \cdot 6$ per cent collector at $\mu = 0 \cdot 10$ and the 10 per cent collector at $\mu = 0 \cdot 05$ reduces η_p by 2 to 3 per cent.

As would be expected these static pressure efficiencies are rather low in comparison with values round 90 per cent measured[4] at low Mach numbers on a simple 5 deg conical diffuser at the same entry Reynolds number of 10^6. The losses have been considered in greater detail in Appendix II and are discussed in section 4.3.2. A feature shown in Fig. 12 is the distortion of the static pressure curves when the collectors were operated at interchange ratios lower than geometrical. It is of interest to note that up to $M = 0 \cdot 8$ no choking occurred at any of the collectors.

4.3.2. *Total head measurements.*—The total head traverses at '*A*' and '*B*' (Figs. 1, 2) in the first diffuser showed no signs of a breakaway of the main flow at the collector for any of the collector entries over the range of interchange ratio tested. There was however, a tendency for the boundary layer on the collector tube to thicken slightly when μ was reduced. Typical curves of total head distribution plotted in the form of total head loss divided by working-section dynamic head are given in Fig. 13.

The total head distribution at the end of the second diffuser showed greater variation and the main results obtained have been plotted in Fig. 14. At the end of the second diffuser the wake from the collector still persists, giving a central hump in the loss distribution. As μ is reduced the losses increase, more particularly at the walls and centre giving a more peaky total head distribution. At a given interchange ratio the losses were greater for the larger collector entries, the difference being spread fairly uniformly over the cross-section. The total head loss coefficient $\eta_H = (H_a - \bar{H})/\frac{1}{2}\rho_0 V_0^2$ has been obtained by integrating the loss distribution curves and the values obtained have been plotted in Fig. 17. This figure also shows loss coefficients calculated for incompressible flow by a semi-empirical method outlined in Appendix II. The measured and calculated losses are in satisfactory agreement indicating that no abnormal losses were

6

occurring. The analysis of losses estimated for the partial model of the tunnel with 15 per cent interchange, working at geometrical interchange ratio is as-follows:—

Section of partial model of tunnel	Loss coefficient $= \dfrac{\Delta H}{\frac{1}{2}\rho_0 V_0{}^2}$ or $\dfrac{\Delta p}{\frac{1}{2}\rho_0 V_0{}^2}$	
	Estimated	Measured
Contraction cone and working-section	0·028	
First diffuser	0·102	
Constant area length between first and second diffuser	0·0095	
Second diffuser	0·012	
Collector supports and interchange air aerofoil ducts	0·004	
Total	0·156	0·154

Some difficulty was encountered in obtaining satisfactory readings of total head at the end of the second diffuser due to fluctuation in reading amounting in some cases to ± 10 per cent of the local dynamic head. This was thought at first to be due to a breakaway in the diffuser, but tufts showed no flow reversals. The most likely cause was the entry into the tunnel of random vortex motions present in the atmosphere. Such motions could not be detected at the entrance to the contraction cone, but at high Mach numbers where some mist formed at the downstream end of the working section, slight random vorticity could be seen at this section. A similar phenomenon was noticed by Squire[4] in tests on conical diffusers operated by a suction plant. In his case the fluctuations disappeared when the tests were repeated using a blower compressor drive.

Pearcey[5] has shown that on expansion of atmospheric air there is a loss of total head associated with condensation of water vapour which however only becomes appreciable above $M = 0.8$.

At $M = 0.8$ the loss in total head is of the order of $\frac{1}{2}$ to 1 in. water gauge which represents at most 1 per cent of the working-section dynamic head. For this reason the main tests were limited to tests at $M = 0.8$ and below. No corrections for this effect have been applied.

4.3.3. *Effect of model in working-section.*—An aerofoil spanning the working-section had very little effect on the flow regime in the tunnel, the efficiencies being only slightly decreased. The static pressure gradient across the diffuser caused by the deflection of the flow round the model became zero by the time the air reached the end of the first diffuser. A comparison between the efficiency of the empty tunnel, and that with the model installed at various incidences, is shown in Table 3.

4.4. *Interchange Collector Duct.*—Fig. 18 shows the variation of total head loss up to the outlet of the interchange aerofoil ducts in terms of the working section dynamic head, for each collector entry, with variation of interchange ratio and Mach number.

7

It is seen that with the shapes of collector entries used, (Fig. 3) the total head losses increased substantially with the smaller entries, working at geometrical interchange ratio. This was due to the larger amount of breakaway taking place on the concave inner walls, and could be improved by the fitting of internal liners, to reduce the rate of diffusion just inside the entry. However, time did not allow these possibilities to be investigated.

Reducing the interchange ratio below geometrical, decreased the amount of breakaway. The slowing up of the air in front of the collector entry caused the stream tubes to expand and hence reduced the incidence of the collector walls relative to the air.

Fig. 15 shows typical total head loss distribution curves at $M_0 = 0 \cdot 6$, for the three collector entries working at geometrical interchange ratio. Fig. 4 shows the positions of the traverses relative to the interchange aerofoil duct cross-section.

The static pressure gradient across the aerofoil ducts leading the interchange air out of the tunnel was small under all conditions, indicating that the thin, sheet metal turning vanes, used for deflecting the air out of the collector tube (Fig. 2) were functioning correctly.

With the $15 \cdot 6$ per cent collector entry fitted, the total head variation across the aerofoil ducts was of the order of 30 per cent of the working-section dynamic head, the largest losses occurring at the leading edge, the air in this section having lost energy in the boundary layer formed on the walls of the collector duct.

When the smaller entries were fitted, however, the breakaway was sufficiently large to spread across the whole of the collector duct, causing an increase in the total head loss, but a greater uniformity in the total head distribution.

The influence of the model in the working-section on the losses in the interchange flow was much more marked than on the main flow, since the low energy air in the aerofoil wake formed a much greater percentage of the interchange flow than it did of the main flow.

A comparison between the total head losses associated with the model in the tunnel at various incidences, and those for the empty tunnel is shown in Table 3.

This shows that introduction of the aerofoil at 0 deg incidence into the tunnel, increases the loss of total head of the interchange air at exit from the tunnel, from 13 per cent to 18 per cent of tunnel dynamic head. At 10 deg incidence and $M = 0 \cdot 2$, and at 5 deg the loss increased from 13 to 30 per cent. Fig. 19 shows that with the tunnel empty, the pressure difference between the inner and outer walls of the collector entry was nearly a linear function of interchange ratio, for any given Mach number. Thus, by means of this simple measurement, an approximate estimate of the interchange ratio was available. No tests were carried out to determine the effect of a model in the working-section, on the pressure difference.

4.5. *Power Required to Extract Interchange Air.*—In Appendix III it is shown that the power required to extract the interchange air from a sub-atmospheric tunnel can be expressed in the form:—

$$H.P. = \frac{\rho_0 A_0 V_0 \mu C_p T_T}{550 \, \eta_c} \left\{ \left[\frac{p_a}{p_0} \left(\frac{1}{(1 + 0 \cdot 2 \, M_0^2)^{3 \cdot 5} - 0 \cdot 7 \, \eta_{H2} \, M_0^2} \right) \right]^{(\gamma - 1)/\gamma} - 1 \right\}$$

From which it can be seen that if η_{H2} is small, the power required, for given working-section conditions, varies directly as the interchange ratio μ.

8

A large reduction in the power required should, therefore, be gained by using the smaller collector entries, provided that the losses in the smaller entries do not rise appreciably compared to those in the 15·6 per cent collector. An example is considered in detail in Appendix III.

5. *Conclusions.*—The tests on the partial model of the engine altitude-tunnel have demonstrated that the interchange air collector designed, can operate up to interchange ratios of the order of 15 per cent without interfering appreciably with the flow in the tunnel working-section. The total head losses in the main tunnel flow are however appreciable since the collector duct has to be in a part of the tunnel where the speed is only slightly lower than in the working-section. These losses are of the order to be expected, and the main flow round the collector was satisfactory, but in a return circuit tunnel screens in the tunnel maximum section would probably be required to remove the 'shadow' of the collector.

Expressed in terms of the tunnel power factor the losses in the main flow due to the interchange collector are of the order ΔP.F. $= 0·05$, so that the interchange system would necessitate an increase in the fan power of a normal wind tunnel of the order of 20 to 30 per cent.

With the 15 per cent interchange system as designed lower air interchange ratios can be obtained by reducing the compression ratio of the exhausting compressors or by installing smaller interchangeable collector entries. The first method is better in cases where it is important to reduce the power requirements of the exhausting compressors, the second is preferable where it is more important to keep the main tunnel fan power to a minimum.

REFERENCES

No.	Author	Title, etc.
1	W. S. Emerson and A. D. Young	High Speed Flow in Slowly Convergent and Divergent Pipes and Channels. R.A.E. Report No. Aero. 1957. July, 1944. A.R.C. 8059. (Unpublished.)
2	—	*Flow Measurement.* B.S.S. 1042.
3	C. B. Millikan, J. E. Smith and R. W. Bell	High Speed Testing in the Southern California Co-operative Wind Tunnel. Paper read before the Anglo-American Aeronautical Conference, London. September, 1947.
4	H. B. Squire	Experiments on Conical Diffusers. R.A.E. Report No. Aero. 2216. August, 1947. A.R.C. 12,838. (Unpublished.)
5	H. H. Pearcey	The Effect of Condensation of Atmospheric Water Vapour on Total Head and Other Measurements in N.P.L. High Speed Tunnel. R. & M. 2249. February, 1944.
6	D. C. MacPhail, D. E. Lindop and E. E. Regan	Tables for Compressible Air Flow Calculations. Part I, Tech. Note No. Aero. 1738. December, 1945. Part II, Tech. Note No. Aero. 1738a. March, 1946. A.R.C. 9743 and A.R.C. 9933. (Unpublished.)
7	H. Glauert	*Aerofoil and Airscrew Theory.*

NOTATION

p		Static pressure
H		Total head
$\bar{H}$		Mean total head $= \int VH dA \Big/ \int V dA$
M		Mach number
A		Area
a		Velocity of sound
T		Absolute temperature, deg C
V		Velocity
$\bar{V}$		Mean velocity
γ	$=$	$C_p/C_v = 1 \cdot 4$
μ		Interchange ratio $= \dfrac{\text{interchange mass flow}}{\text{working-section mass flow}}$
μ_G		Geometrical interchange ratio $\left[\dfrac{\text{collector entry diameter}}{\text{diffuser shell diameter in plane of entry}}\right]^2$
R		Gas constant
ρ		Density
η_H		Total head loss coefficient $= (H_a - \bar{H})/\frac{1}{2}\rho_0 V_0^2$
η_p	$=$	$\dfrac{\text{Actual static pressure recovery}}{\text{Ideal static pressure recovery}} = (p - p_0)/(p_i - p_0)$
η_C		Exhausting compressor adiabatic efficiency
S		Cross-sectional area of tunnel or pipe
δ^*		Boundary-layer displacement thickness
Suffix 0		denotes reference plane values
1		end of second diffuser
2		outlet of interchange aerofoil ducts
a		atmospheric conditions
e		entry traverse position
e_c		centre of entry traverse
c'		outer wall of collector entry
c''		inner wall of collector entry
x		plane of H.I.S.(1)
y		plane of H.I.S.(2)
i		ideal adiabatic frictionless flow
T_T		total temperature

10

APPENDIX I

Tunnel Calibration

Preliminary calibration tests were made as listed below:—

(1) *Measurement of the Total Head and Velocity Distributions across the Working-Section and Across the Entry to the Tunnel.*—Pitot and static pressure traverses made in both the horizontal and vertical plane across the working-section showed that both the total head and static pressure were uniform, over the speed range $M = 0 \cdot 2$, to $M = 0 \cdot 8$, within the accuracy of measurement, *i.e.*, $\frac{1}{2}$ per cent of the working-section dynamic head, the total head being equal to atmospheric pressure.

Traverses in the entry showed that the total head distribution across the section was uniform, and equal to atmospheric pressure. The velocity distribution across the entry is shown in Fig. 5.

(2) *Calibration of the Mach number at a Reference Plane in the Working-Section as a Function of Two Arbitrary Wall Static Pressures in the Contraction Cone, one in the Maximum Section, and the other just Upstream of the Beginning of the Working-Section. H.I.S.(1) and H.I.S.(2) respectively.*—The nominal working-section Mach numbers quoted, refer to a reference plane $0 \cdot 2$ working-section diameters downstream of the beginning of the working-section. Since the working-section total head was equal to atmospheric pressure, and the static pressure across the working-section was uniform, the nominal Mach numbers of tests could be computed from the relation

$$\frac{p_0}{H_0} = \left(1 + \frac{\gamma - 1}{2} M_0^2\right)^{\gamma/(\gamma - 1)} \qquad \text{..} \qquad \text{..} \qquad \text{..} \qquad \text{..} \qquad \text{..} \qquad (1)$$

Tables for Compressible Air Flow[6] being used to reduce the computations.

This method of obtaining nominal Mach number could not be used when a model was in the working-section or if the collector was likely to interfere with working-section static pressures. Following normal tunnel technique M_0 was calibrated against $(p_x - p_y)/p_x$ where p_x and p_y are the two hole-in-side wall pressures.

(3) *Calibration of the Mass Flow of Air Entering the Tunnel in Terms of Atmospheric Temperature and Pressure and the Reference Mach number.*—In order to obtain a value for μ, the interchange ratio for each test run, it was necessary to know the total tunnel mass flow and the interchange air mass flow. The latter was calculated from the standard nozzle characteristics, the former could be estimated from atmospheric conditions and the reference Mach number assuming isentropic flow in the contraction cone. It was decided, however, to check the total tunnel flow by traverses at entry since the error due to assuming ideal flow was uncertain.

Theoretical Mass Flow.—Assuming frictionless adiabatic flow, the mass flow in the tunnel can be expressed in terms of the atmospheric conditions and the reference Mach number in the working-section.

For
$$H_0 = p_a, \qquad \text{..} \qquad \text{..} \qquad \text{..} \qquad \text{..} \qquad \text{..} \qquad \text{..} \qquad \text{..} \qquad (2)$$

$$T_{0,T} = T_a \qquad \text{..} \qquad \text{..} \qquad \text{..} \qquad \text{..} \qquad \text{..} \qquad \text{..} \qquad \text{..} \qquad (3)$$

$$\frac{T_a}{T_0} = 1 + \frac{\gamma - 1}{2} M_0^2 \qquad \text{..} \qquad \text{..} \qquad \text{..} \qquad \text{..} \qquad \text{..} \qquad (4)$$

11

$$\frac{p_0}{\rho_0 T_0} = R \qquad \qquad \dotsc \quad \dotsc \quad \dotsc \quad \dotsc \quad \dotsc \quad \dotsc \qquad (5)$$

$$\frac{p}{\rho^\gamma} = \text{const.} \qquad \dotsc \quad \dotsc \quad \dotsc \quad \dotsc \quad \dotsc \quad \dotsc \qquad (6)$$

$$a^2 = \frac{\gamma p}{\rho} = \gamma RT, \qquad \dotsc \quad \dotsc \quad \dotsc \quad \dotsc \quad \dotsc \quad \dotsc \qquad (7)$$

and

$$\tfrac{1}{2}V_0^2 + \frac{\gamma}{\gamma - 1}\frac{p_0}{\rho_0} = \frac{\gamma}{\gamma - 1}\frac{p_a}{\rho_a} \qquad \dotsc \quad \dotsc \quad \dotsc \quad \dotsc \quad \dotsc \qquad (8)$$

whence

$$\rho_0 A_0 V_0 = \frac{p_0}{RT_0} M_0 A_0 \sqrt{\left(\frac{\gamma R T_a}{1 + \dfrac{\gamma - 1}{2} M_0^2}\right)} \qquad \dotsc \quad \dotsc \quad \dotsc \quad \dotsc \qquad (9)$$

$$= \frac{A_0}{\sqrt{R}}\frac{a}{\sqrt{T_a}} M_0 \sqrt{\gamma} \left[\frac{1}{1 + \dfrac{\gamma - 1}{2} M_0^2}\right]^{(1 + \gamma)/2(\gamma - 1)} \qquad \dotsc \quad \dotsc \quad \dotsc \quad \dotsc \qquad (10)$$

Measured Mass Flow.—The measured mass flow was obtained from the two pitot static traverses at right-angles at the tunnel entry by integrating over the entry area.

Comparison of Measured and Theoretical Mass Flows.—The measured and theoretical mass flows and their ratios are given in the table below:—

	Horizontal Traverse					Vertical Traverse		

M_0	Mass Flow (slugs/sec)		$\dfrac{\text{Measured}}{\text{Theoretical}}$		M_0	Mass Flow (slugs/sec)		$\dfrac{\text{Measured}}{\text{Theoretical}}$
	Theoretical	Measured				Theoretical	Measured	
0·806	0·830	0·844	1·02		0·897	0·825	0·804	0·971
0·755	0·819	0·843	1·03		0·797	0·804	0·778	0·967
0·691	0·780	0·741	1·03		0·708	0·768	0·748	0·974
0·674	0·771	0·801	1·03		0·299	0·410	0·398	0·971
0·457	0·500	0·615	1·03					
0·341	0·474	0·484	1·02				Mean Value	0·971
		Mean Value	1·03					

The mean value of the ratio Measured Mass Flow/Theoretical Mass Flow from the two traverses was 1·00 within the limits of experimental error. In the tests, therefore, the total mass flow was calculated using the theoretical expression without correction.

APPENDIX II

Estimation of Total Head Losses in the Partial Model

Assuming incompressible flow throughout, and a working-section Reynolds number of 2×10^6

Losses were derived by graphical integration along the tunnel of the losses in elemental cylindrical and annular sections in terms of the working-section dynamic head.

Circular Sections

$$\frac{d(\Delta H)}{\frac{1}{2}\rho_0 V_0^2} = (1 - \mu)^2 \frac{A_0^2}{A^2} \frac{\lambda}{D} dx \qquad .. \qquad .. \qquad .. \qquad .. \qquad .. \qquad (11)$$

Annular Sections

$$\frac{d(\Delta H)}{\frac{1}{2}\rho_0 V_0^2} = (1 - \mu)^2 \frac{A_0^2}{A_1^2} \frac{(D_1^2 - d_1^2)^2}{(D^2 - d^2)^2} \frac{\lambda}{D - d} dx \qquad .. \qquad .. \qquad .. \qquad .. \qquad (12)$$

where $D - d$ hydraulic mean diameter at element considered,

D_1 outer shell diameter at beginning of annular diffuser,

d_1 inner shell diamater at beginning of annular diffuser,

D outer shell diameter at element considered,

d inner shell diameter at element considered,

A_1 area of X-section at beginning of annular diffuser,

A area of X-section of element of annular diffuser,

$\lambda = 4C_f$, where C_f is the skin friction coefficient,

dx length of element of diffuser,

ΔH total head loss in partial model.

All other symbols as defined in notation.

Determination of λ.—For the contraction cone, working-section, and constant area section between the first and second diffusers, λ was derived from the Kármán relation for turbulent flow in smooth pipes

$$\frac{1}{\sqrt{\lambda}} = 2 \log_{10} (R.N. \sqrt{\lambda}) - 0\cdot8 \qquad .. \qquad .. \qquad .. \qquad .. \qquad .. \qquad (13)$$

where $R.N.$ is the Reynolds number based on pipe diameter or hydraulic mean diameter. For the diffusers, experimental values of λ were used, since the skin friction coefficient is increased in the presence of an adverse pressure gradient.

These values were obtained from tests by Squire[4] on conical diffusers, for the same cone angle, or in the case of annular diffusers for the equivalent conical diffuser angle.

The results in Ref. 4 are given in the form

$$\eta_p = \frac{p_2 - p_1}{p_{2i} - p_1}$$

for varying cone angles at constant entry Reynolds number.

13

Therefore
$$\frac{\Delta H}{\frac{1}{2}\rho_1 V_1^2} = (1 - \eta_p)\left(1 - \frac{A_1^2}{A_2^2}\right) \quad .. \qquad .. \qquad .. \qquad .. \qquad .. \tag{14}$$

Integrating equation (11) for a conventional diffuser

$$\frac{\Delta H}{\frac{1}{2}\rho_1 V_1^2} = \frac{\lambda}{8 \tan \alpha/2}\left[1 - \frac{D_1^4}{D_2^4}\right] \quad .. \qquad .. \qquad .. \qquad .. \qquad .. \tag{15}$$

where α total cone angle of diffuser,
D_1 diameter at entry of diffuser,
D_2 diameter at exit of diffuser.

Therefore substituting equation (14) into equation (15)

$$\lambda = 8(1 - \eta_p)\tan \alpha/2 . \qquad .. \qquad .. \qquad .. \qquad .. \qquad .. \tag{16}$$

Losses at collector supports and aerofoil ducts

Assuming $C_D = 0\cdot01$ for a symmetrical aerofoil

$$\frac{\Delta H}{\frac{1}{2}\rho_0 V_0^2} = C_D S \frac{A_0^2}{A^2}(1 - \mu)^2 \quad .. \qquad .. \qquad .. \qquad .. \qquad .. \tag{30}$$

where S area in plan view of supports,
A area of duct at support.

Summary of Losses

$$\Delta H / \tfrac{1}{2}\rho_0 V_0^2$$

μ	15·6 per cent Collector			10 per cent Collector		
	0·12	0·156	0·20	0·05	0·07	0·10
Section						
Contraction Cone	0·0113	0·0113	0·0113	0·0113	0·0113	0·0113
Working-Section	0·0167	0·0167	0·0167	0·0167	0·0167	0·0167
First Diffuser	0·1100	0·1023	0·0933	0·1219	0·1171	0·1097
Constant Area Duct	0·0102	0·0094	0·0085	0·0119	0·0114	0·0107
Second Diffuser	0·0131	0·0121	0·0109	0·0152	0·0147	0·0137
Collector Supports and Aerofoil Ducts	0·0046	0·0042	0·0038	0·0053	0·0051	0·0048
Total	0·1659	0·1560	0·1445	0·1823	0·1763	0·1669
First and Second Diffusers	0·1231	0·1144	0·1042	0·1371	0·1318	0·1234

14

Power Required to Extract Interchange Air from a Tunnel

$$\text{H.P. required} = \frac{\rho_0 A_0 V_0 \mu C_p \cdot T_T}{550\, \eta_c} [r^{(\gamma-1)/\gamma} - 1] \text{ assuming adiabatic compression,} \qquad \text{..} \quad (33)$$

where r pressure ratio $\qquad = \dfrac{p_{at}}{H_2}$ $\qquad$ .. $\qquad$ .. $\qquad$ .. $\qquad$ .. $\qquad$ .. $\qquad$ .. $\quad$ (34)

But $\qquad\qquad\qquad\qquad H_0 - H_2 = \eta_{H2} \tfrac{1}{2} \rho_0 V_0^2 .$ $\qquad$ .. $\qquad$ .. $\qquad$ .. $\qquad$ .. $\qquad$ .. $\quad$ (35)

Therefore $\qquad\qquad\qquad H_2 = H_0 - \eta_{H2} \tfrac{1}{2} \rho_0 V_0^2 .$

Therefore $\qquad\qquad\qquad r = \dfrac{p_{at}}{H_0 - \eta_{H2}} \tfrac{1}{2}\rho_0 V_0^2 .$ $\qquad$ .. $\qquad$ .. $\qquad$ .. $\qquad$ .. $\qquad$ .. $\quad$ (36)

But $H_0 = p_0(1 + 0\cdot2\,M_0^2)^{3\cdot5}$ from equation (1).

Therefore $\qquad r^{(\gamma-1)/\gamma} = \left\{ \dfrac{p_{at}}{p_0(1 + 0\cdot2M_0^2)^{3\cdot5} - \eta_{H2}\, 0\cdot7 p_0 M_0^2} \right\}^{(\gamma-1)/\gamma}$

$$= \left[\frac{p_{at}}{p_0} \left\{ \frac{1}{(1 + 0\cdot2M_0^2)^{3\cdot5} - 0\cdot7\eta_{H2}M_0^2} \right\} \right]^{0\cdot2857} \qquad \text{..} \quad \text{..} \quad (37)$$

Therefore H.P. required $= \dfrac{\rho_0 A_0 V_0 \mu C_p \cdot T_T}{550\eta_c} \left[\left(\dfrac{p_{at}}{p_0} \left\{ \dfrac{1}{(1 + 0\cdot2M_0^2)^{3\cdot5} - 0\cdot7\eta_{H2}M_0^2} \right\} \right)^{0\cdot2857} - 1 \right]$ $\quad$ (38)

For tunnels running at altitude pressures this compressor power required to extract the interchange air can be very large. It will be noted from equation (38) that at given working-section pressure and temperature, the interchange compressor power is a function of the interchange ratio μ, the losses in the collector η_{H2}, and the Mach number.

Some guide to the relative importance of μ and η_{H2} can be obtained by comparing the interchange power for $\mu = 15$ per cent and low duct losses ($\eta_{H2} = 0\cdot2$) with $\mu = 10$ per cent and high duct losses ($\eta_{H2} = 1\cdot0$). This 'power ratio' has been estimated for a range of tunnel pressures and Mach numbers and the results are given below.

10 per cent Collector

Interchange Power Ratio $=$	Interchange H.P. required with 10 per cent Collector ($\eta_{H2} = 1$)			
	Interchange H.P. required with 15 per cent Collector ($\eta_{H2} = 0\cdot2$)			
M_0	0·2	0·4	0·6	0·8
Working Section Altitude Conditions				
Height ft / relative pressure				
0 1·000	*	*	*	*
10,000 0·688	0·6835	0·8453	1·3514	15·523
20,000 0·459	0·6621	0·7297	0·8638	1·1284
30,000 0·300	0·6553	0·6992	0·7768	0·8974
40,000 0·185	0·6517	0·6842	0·7386	0·8149
50,000 0·114	0·6499	0·6764	0·7195	0·7769

* Interchange air will automatically exhaust to atmosphere due to total head being greater than atmospheric pressure. The values of the interchange power ratio for the 5 per cent entry will be exactly half of those for the 10 per cent entry.

In this example the interchange compressor power is appreciably reduced by lowering the interchange ratio from 15 to 10 per cent in spite of the high losses assumed in the smaller collector, except in cases where both M is high and the pressure is only slightly sub-atmospheric.

APPENDIX IV

Pressure Gradient at the End of a Contraction Cone

In one-dimensional pipe flow

$$\frac{dS}{S} = -\frac{dv}{v}(1 - M^2) \qquad \qquad \qquad \qquad \qquad (39)[7]$$

also

$$\frac{d\rho}{\rho} + \frac{dS}{S} + \frac{dv}{v} = 0, \text{ continuity,} \qquad \qquad \qquad \qquad (40)$$

and

$$\frac{dp}{p} - \gamma\frac{dp}{\rho} = 0, \text{ for isentropic flow.} \qquad \qquad \qquad (41)$$

Hence

$$\frac{1}{\gamma}\frac{dp}{p} + \frac{dS}{S}\left(1 - \frac{1}{1 - M^2}\right) = 0 \qquad \qquad \qquad \qquad (42)$$

and

$$\frac{dp}{dx} = \frac{\gamma p}{S}\frac{M^2}{1 - M^2}\frac{dS}{dx}. \qquad \qquad \qquad \qquad \qquad (43)$$

For a round pipe, radius r,

$$\frac{dS}{dx} = 2\pi r\left(\frac{dr}{dx} - \frac{d\delta^*}{dx}\right) \qquad \qquad \qquad \qquad \qquad (44)$$

and

$$\frac{dp}{dx} = \frac{M^2}{1 - M^2}\frac{2\gamma p}{r}\left(\frac{dr}{dx} - \frac{d\delta^*}{dx}\right). \qquad \qquad \qquad \qquad (45)$$

At the end of a contraction cone $dr/dx = 0$ so that

$$\frac{dp}{dx} = \frac{M^2}{1 - M^2}\frac{2\gamma p}{r}\frac{d\delta^*}{dx}. \qquad \qquad \qquad \qquad \qquad (46)$$

16

Equation (46) would not apply to short contraction cones where the pressure gradient depends also on the curvature of the flow, but it might be expected to apply in better designed contraction cones which have low rates of decrease of area at the downstream end to avoid suction peaks at the wall.

Equation (46) then shows that the growth of the boundary layer might have an appreciable effect on the pressure gradient at entry to the working-section in the case of small tunnels working near $M = 1$.

In the engine altitude model dp/dx over the central half of the working-section is zero, hence from equation (45) $d\delta^*/dx = dr/dx$. Using this value of $d\delta^*/dx$ (0·0025) as a first approximation to the value at the beginning of the working-section the values of dp/dx measured and estimated from equation (46) compare as under:—

M	$\dfrac{dp}{dx}$ Measured	$\dfrac{dp}{dx}$ Calculated
0·25	0·027	0·026
0·82	0·075	0·073
0·89	0·13	0·11

which shows reasonable agreement.

Thus the boundary-layer growth should be taken into account when designing the geometry of contraction cones for small tunnels of the order of 1 to 2-ft diameter when they are to work near $M = 1$.

TABLE 1

Dimensions of Contraction Cone

$\dfrac{x}{r_0}$	$\dfrac{r}{r_0}$
0	1·0
1·0	1·009
1·5	1·041
2·0	1·095
2·5	1·188
3·0	1·340
3·5	1·606
4·0	2·090
4·8	3·032
5·2	3·452
5·6	3·744
6·0	3·932
6·4	4·000

r_0 radius at beginning
of working-section
$= 10·004$ in.

r radius at any point
$\times$ working-section radii
upstream of beginning
of working-section.

TABLE 2

Dimensions of Tunnel

Section	Length	Diameter		Area	
Contraction Cone	32 in.	Beginning	40 in.	1256·640	sq in.
		End	10·004 in.	78·603	,,
Working-Section	16 in.	Beginning	10·004 in.	78·603	,,
		End	10·080 in.	79·802	,,
First Diffuser	39·70 in.	Beginning	10·080 in.	79·802	,,
		End { Outer wall	14·704 in.		
		{ Collector wall	7·353 in.	127·346	,,
Collector Tube	36·58 in.	Internal Beginning { 15 per cent	4·125 in.	13·364	,,
		{ 10 per cent	3·240 in.	8·245	,,
		{ 5 per cent	2·280 in.	4·083	,,
		End	5·470 in.	23·500	,,
Second Diffuser	33·77 in.	Beginning	13·06 in.	133·961	,,
		End	15·97 in.	200·309	,,
Four Interchange Aerofoil Ducts				23·818	,,
I.S.A. Nozzle			6·32 in.	31·371	,,

TABLE 3

Effect of Model in Working-Section on Tunnel Total Head Losses (15·6 *per cent Collector*)

Main Flow

M_0	Model Incidence	$\dfrac{H_a - \bar{H}_1}{\frac{1}{2}\rho_0 V_0{}^2}$	μ
	Tunnel Empty	0·1540	0·1590
0·200	0 deg	0·1770	0·1589
	10 deg	0·1887	0·1589
	Tunnel Empty	0·1540	0·1580
0·5	5 deg	0·1881	0·1507

Interchange Flow

M_0	Model Incidence	$\dfrac{H_a - \bar{H}_1}{\frac{1}{2}\rho_0 V_0{}^2}$	μ
	Tunnel Empty	0·1250	0·1590
0·200	0 deg	0·1775	0·1589
	10 deg	0·3021	0·1585
	Tunnel Empty	0·1300	0·1570
0·5	0 deg	0·1784	0·1570
	5 deg	0·2883	0·1558
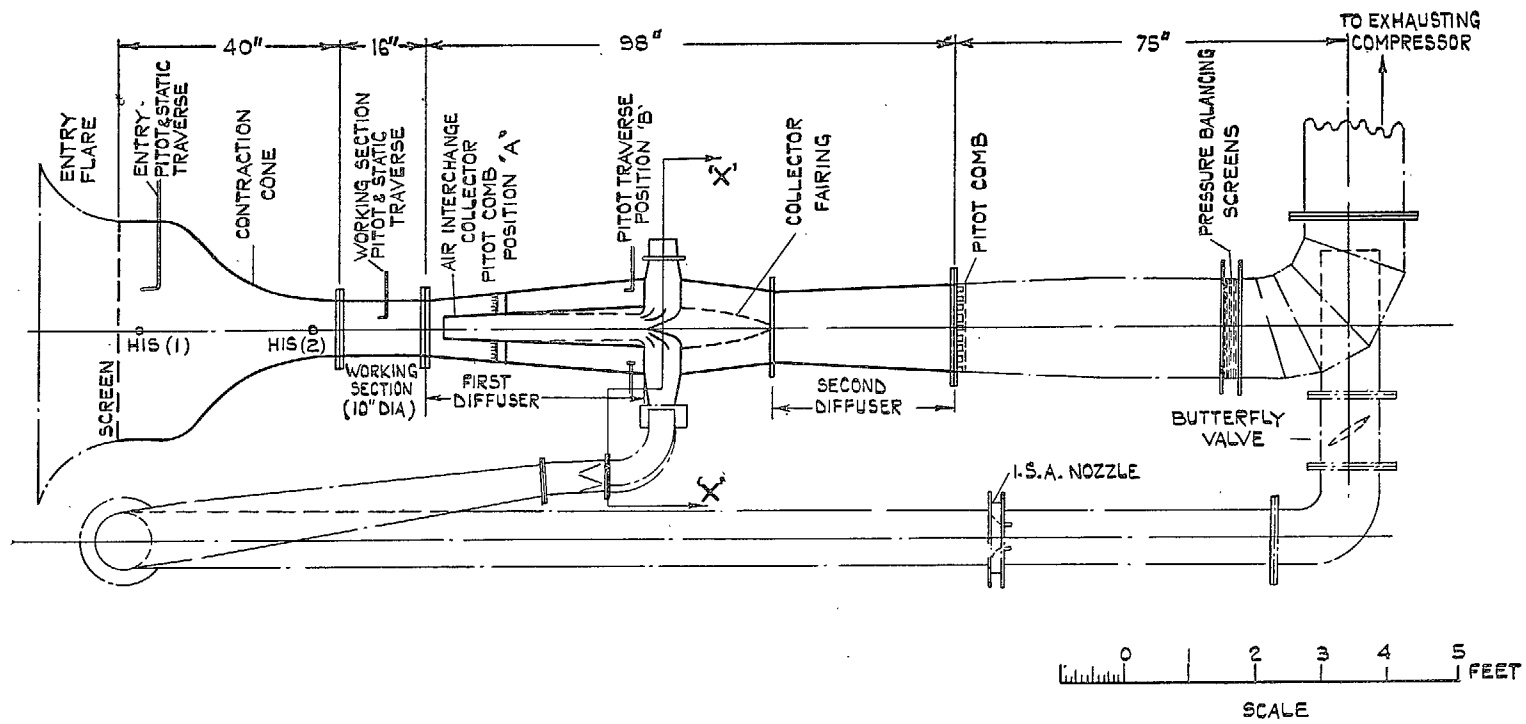
FIG. 1.   General arrangement of partial model of engine altitude-tunnel.
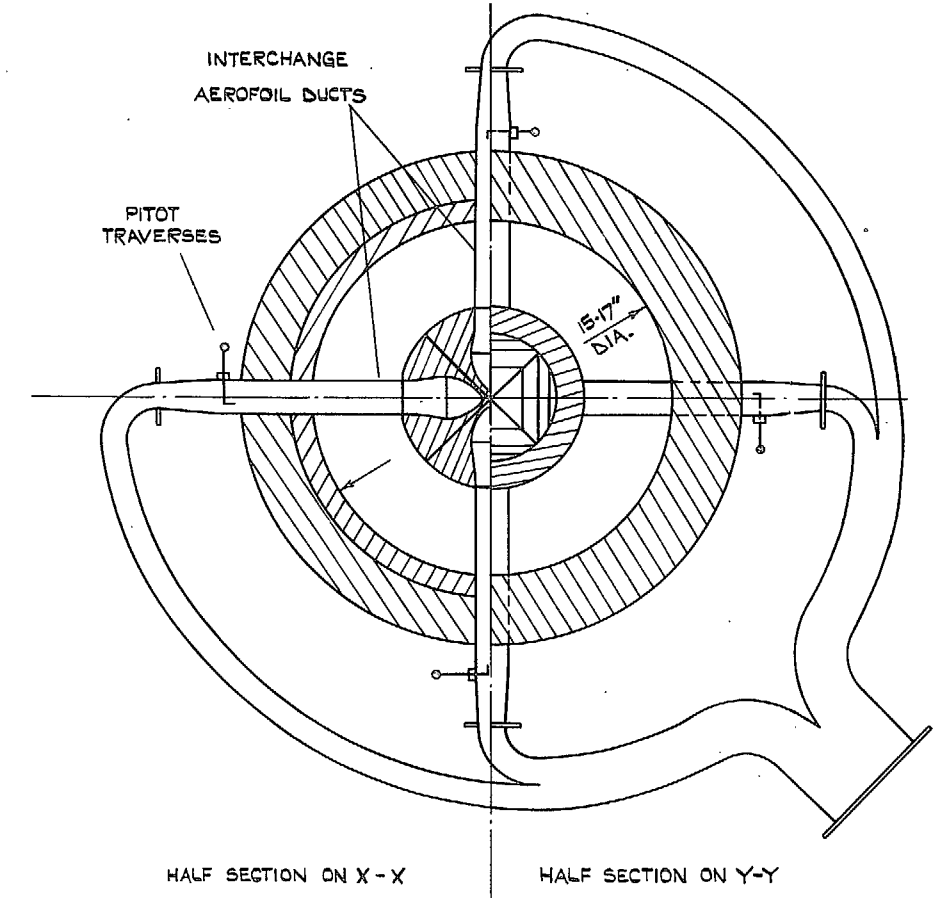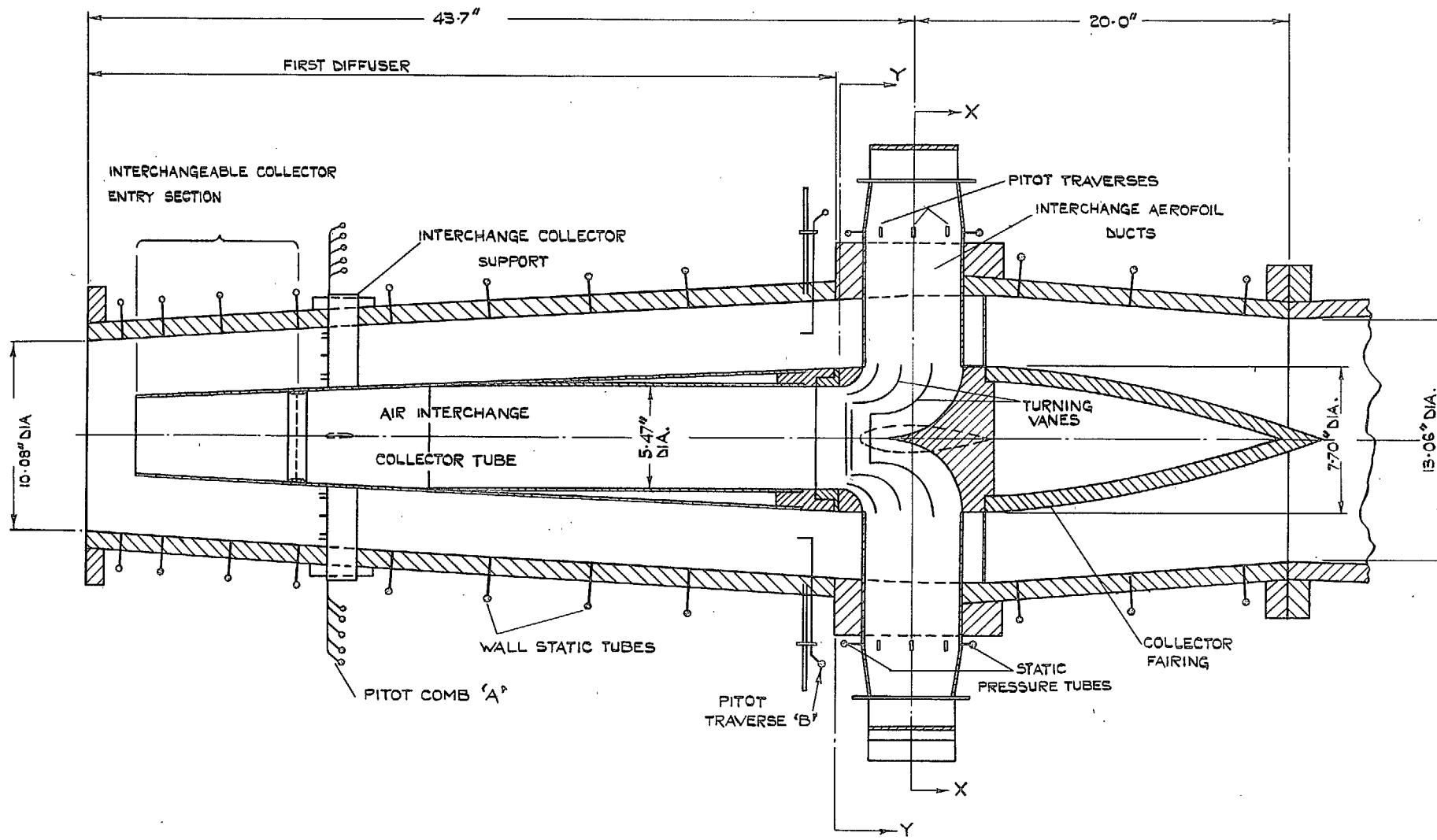
FIG. 2. DETAIL ASSEMBLY OF AIR INTERCHANGE COLLECTOR

HALF SECTION ON X-X   HALF SECTION ON Y-Y

SCALE

4580-15-608-1024-12/51. (M.F.P.)
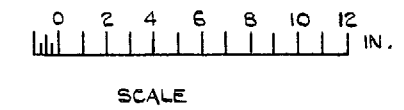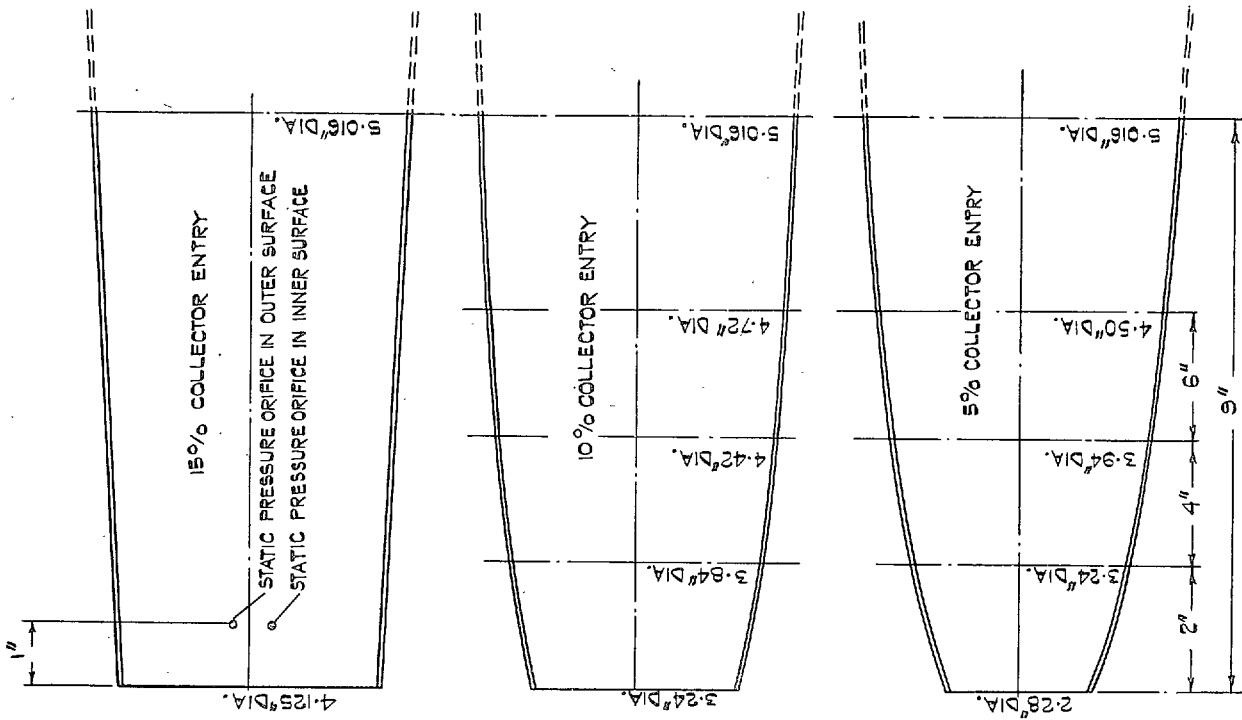
FIG. 3. Geometry of collector entries.

15% COLLECTOR ENTRY

STATIC PRESSURE ORIFICE IN OUTER SURFACE
STATIC PRESSURE ORIFICE IN INNER SURFACE

5·016″ DIA.

4·125″ DIA.

1″

10% COLLECTOR ENTRY

5·016″ DIA.

4·75″ DIA.

4·42″ DIA.

3·84″ DIA.

3·24″ DIA.

5% COLLECTOR ENTRY

5·016″ DIA.

4·50″ DIA.

3·94″ DIA.

3·24″ DIA.

2·82″ DIA.

9″

6″

4″

2″

6·88″

5·50″

2·75″

1·75″

1·75″

STATIC PRESSURE TUBE

STATIC PRESSURE TUBE

TRAILING EDGE FAIRING

TRAVERSE 'C'

TRAVERSE 'D'

TRAVERSE 'E'

0   1   2 IN

SCALE

FIG. 4. Position of total head traverses and wall static pressure tubes in interchange aerofoil ducts.

21
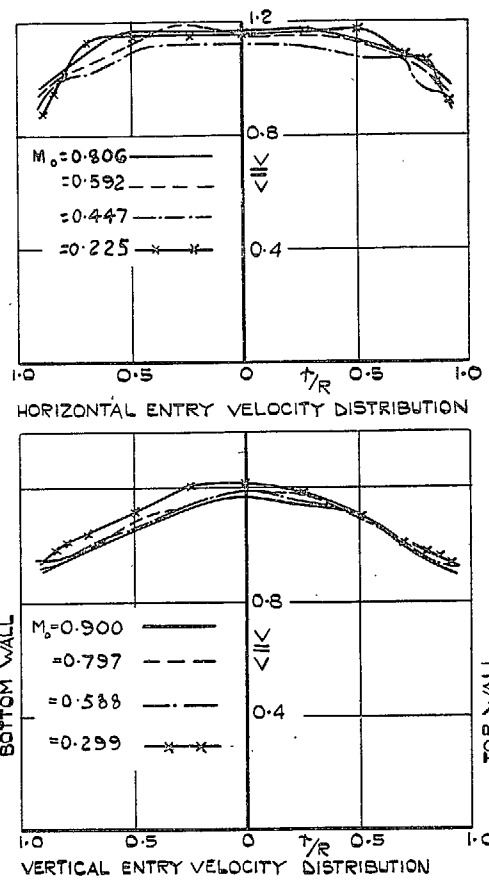
FIG. 5a. Effect of Mach number on entry velocity distributions.
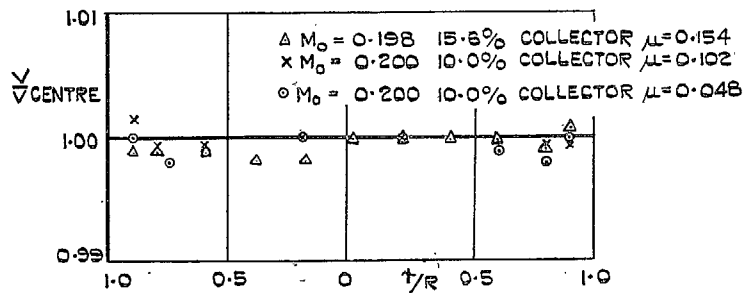
FIG. 5b. Effect of collector size and interchange ratio on velocity distribution across working-section.
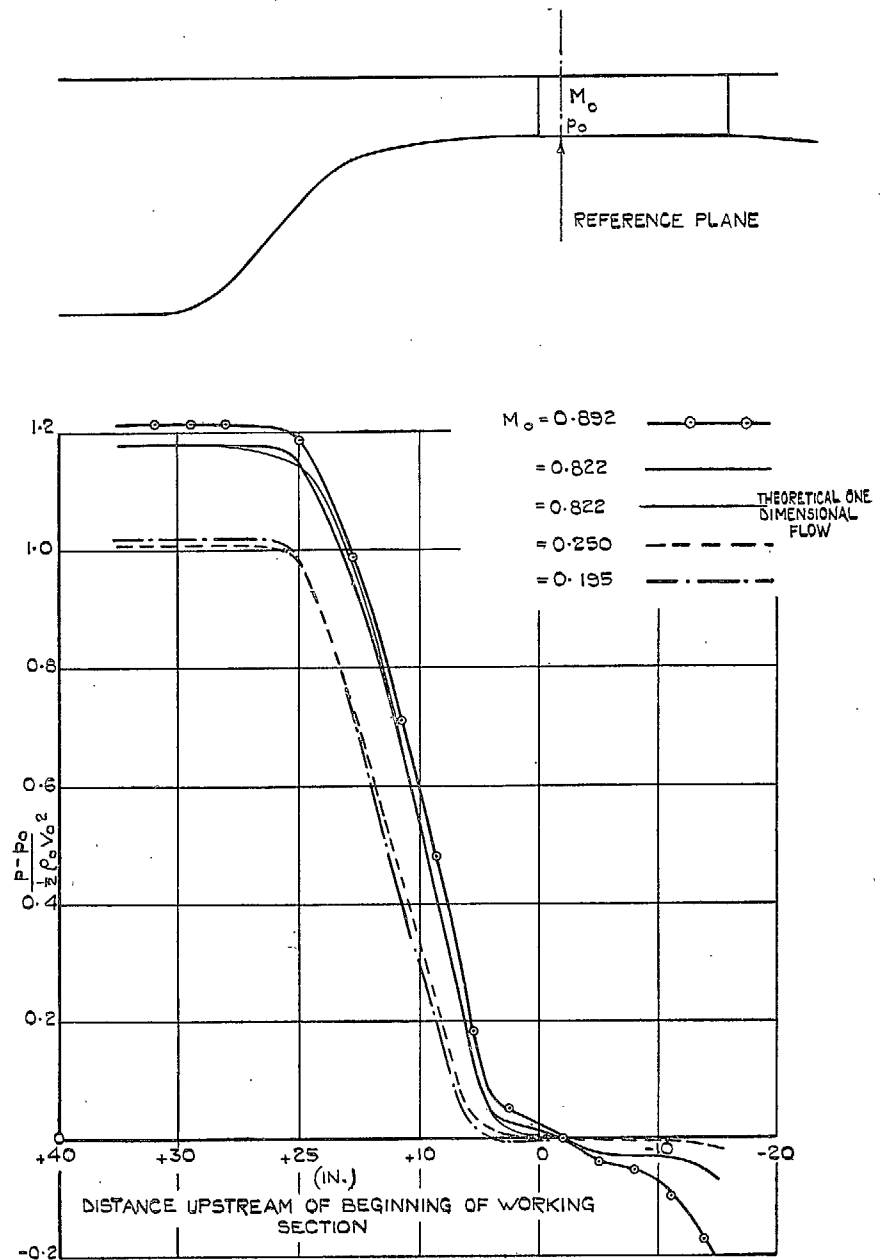
FIG. 6. Wall static pressure distribution down contraction cone.
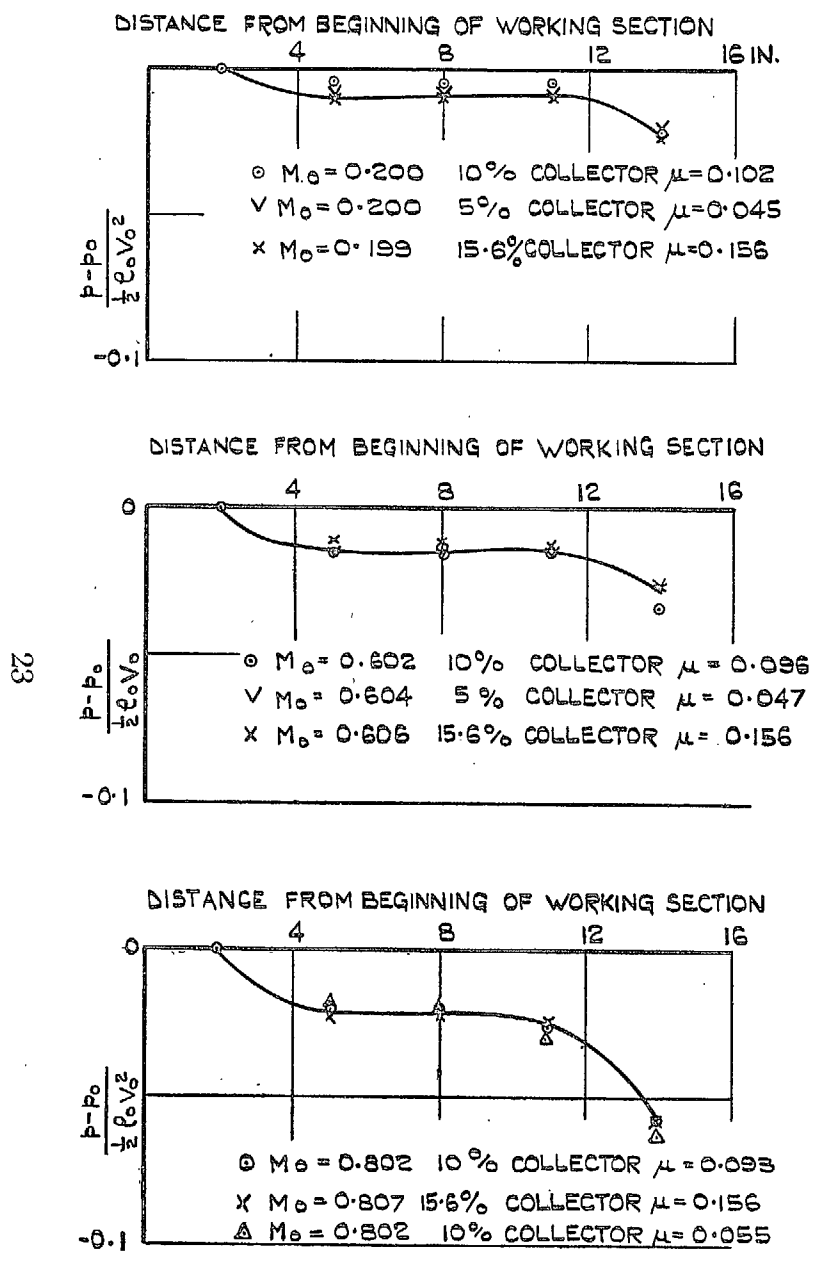
FIG. 7. Effect of variation of collector size and interchange ratio on static pressure variation down working-section walls.
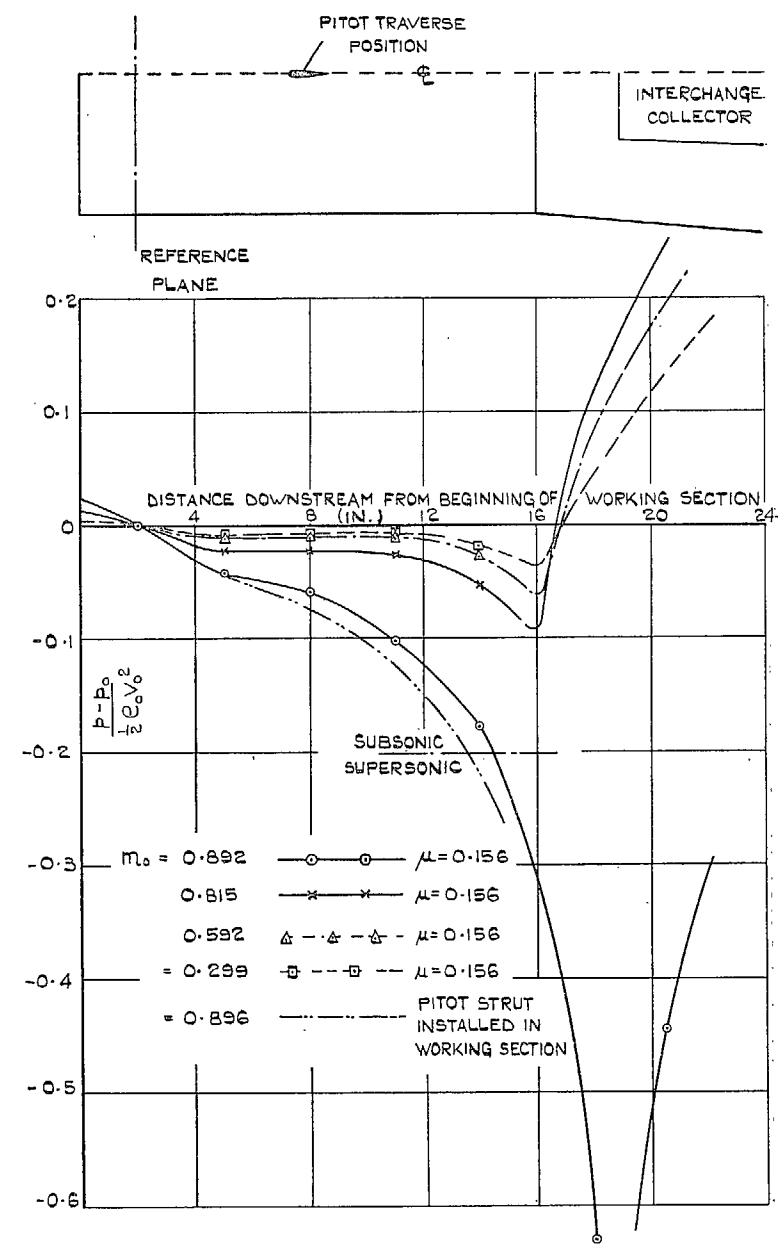
FIG. 8. Wall static pressure variation down working-section (15·6 per cent collector).
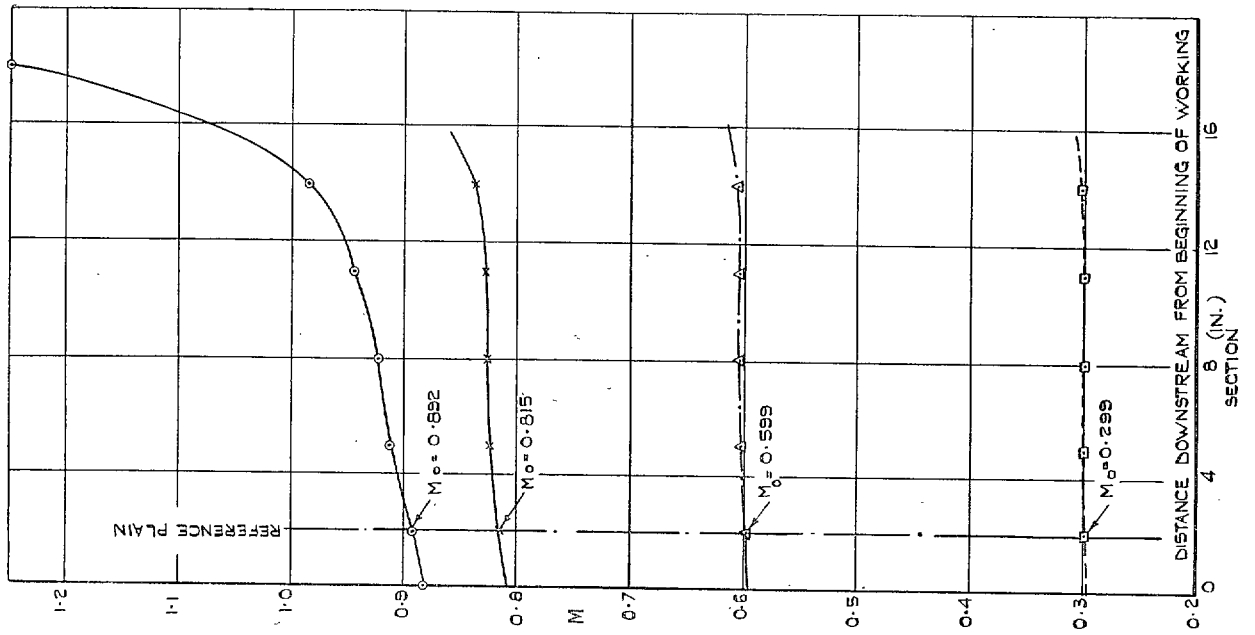
FIG. 9. Mach number variation along working-section (15·6 per cent collector) ($\mu = 0 \cdot 156$).
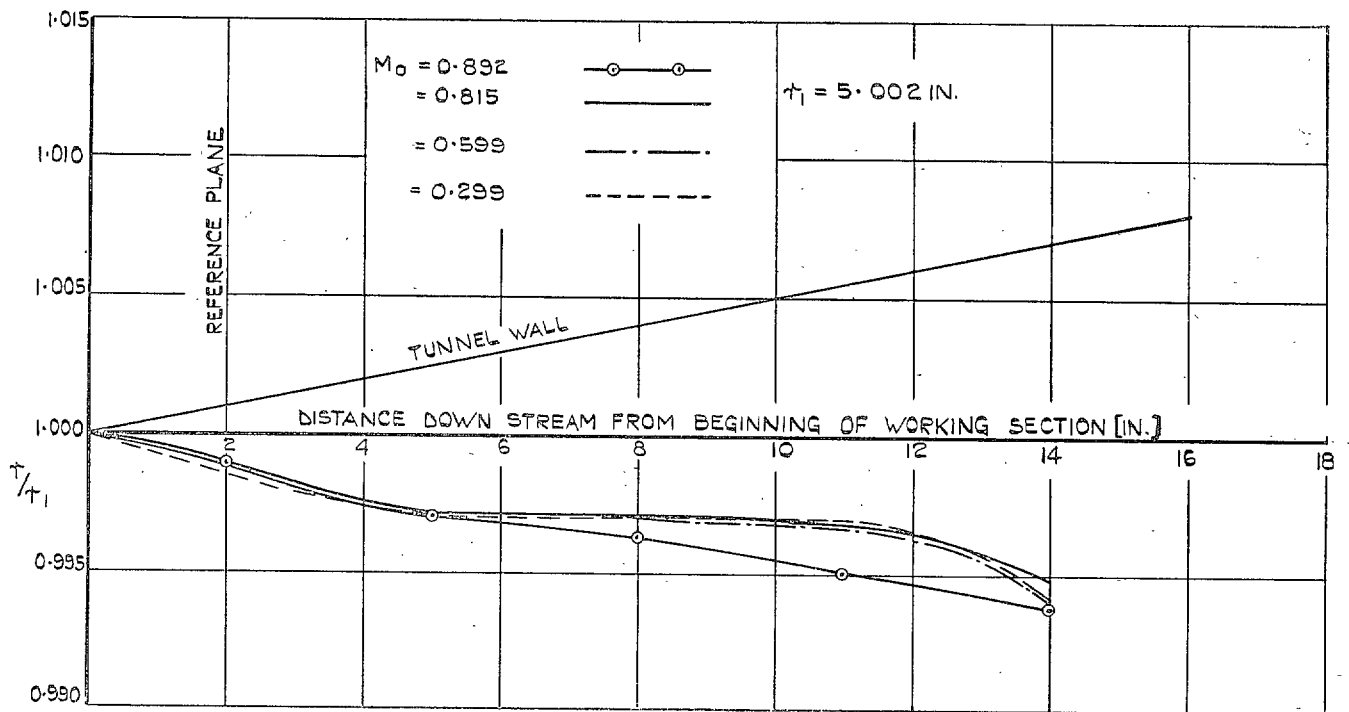
FIG. 10. Variation of effective working-section radius with Mach number (15·6 per cent collector entry) ($\mu = 0 \cdot 156$).

24
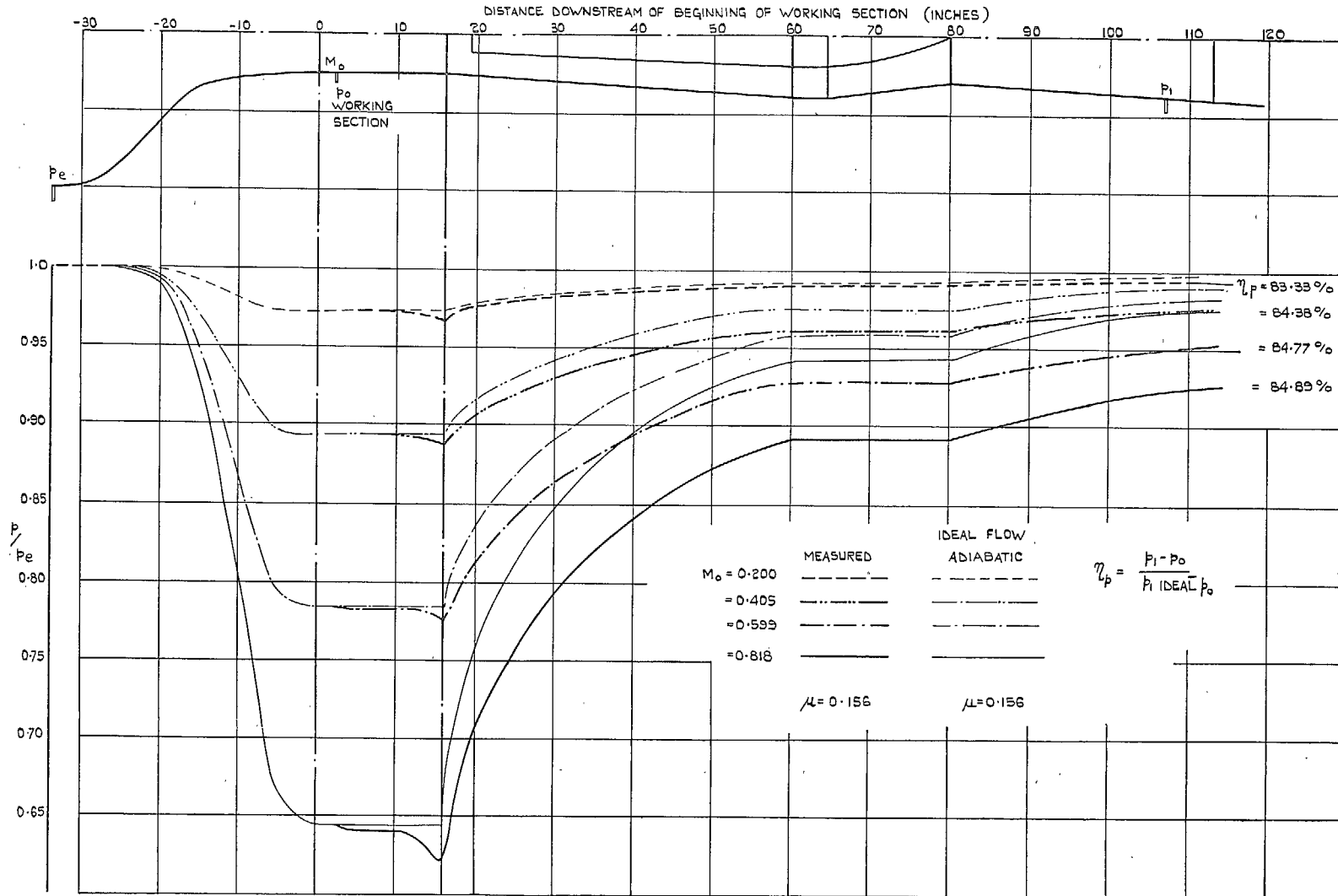
FIG. 11. Effect of Mach number on static pressure distribution along walls of tunnel, and comparison with distribution for ideal adiabatic flow (15·6 per cent collector entry).
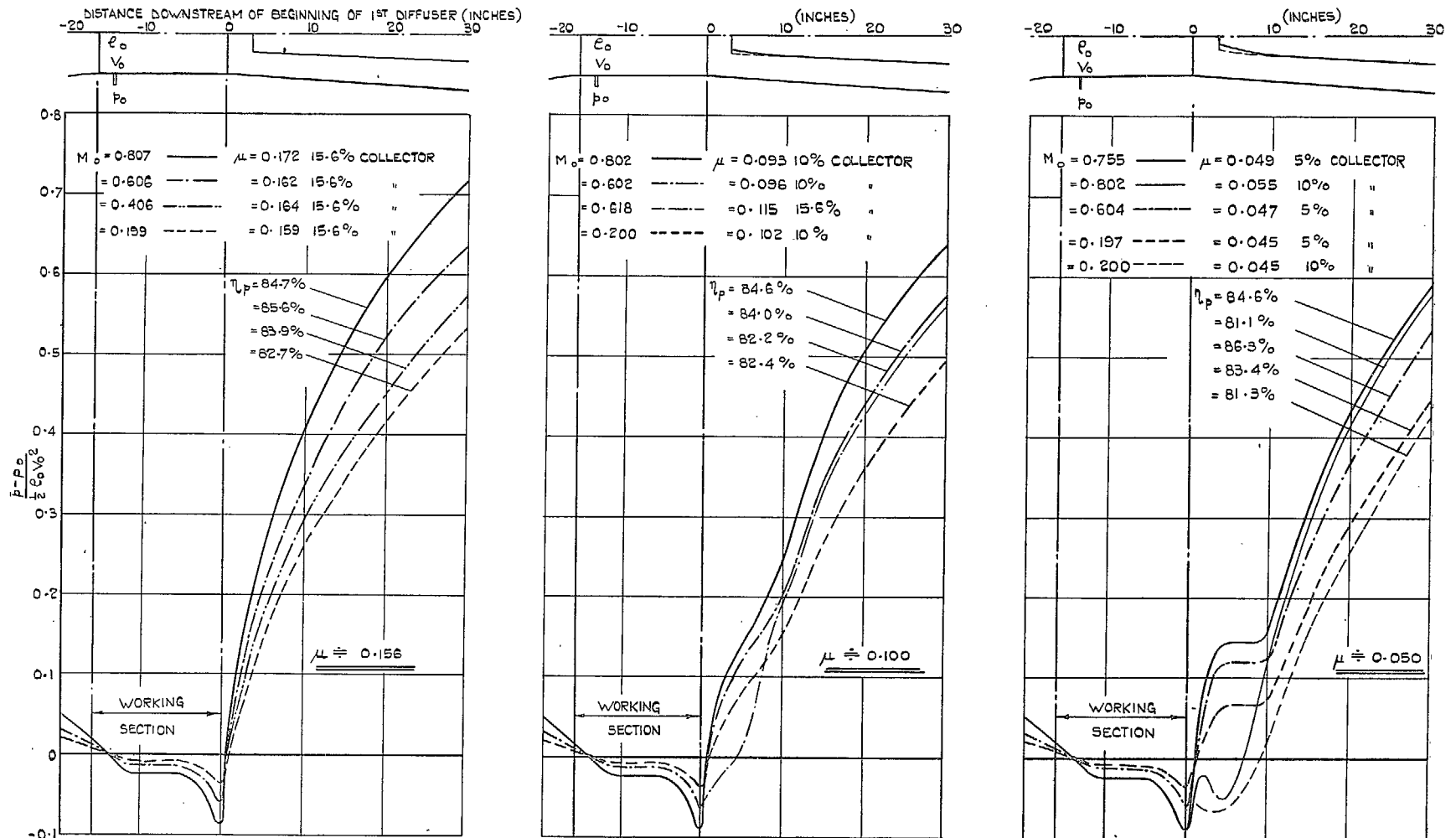
FIG. 12.   Variation of static pressure distribution on walls of working-section and first diffuser with Mach number, interchange ratio (μ) and collector entry size.

TRAVERSE 'A' FIRST DIFFUSER
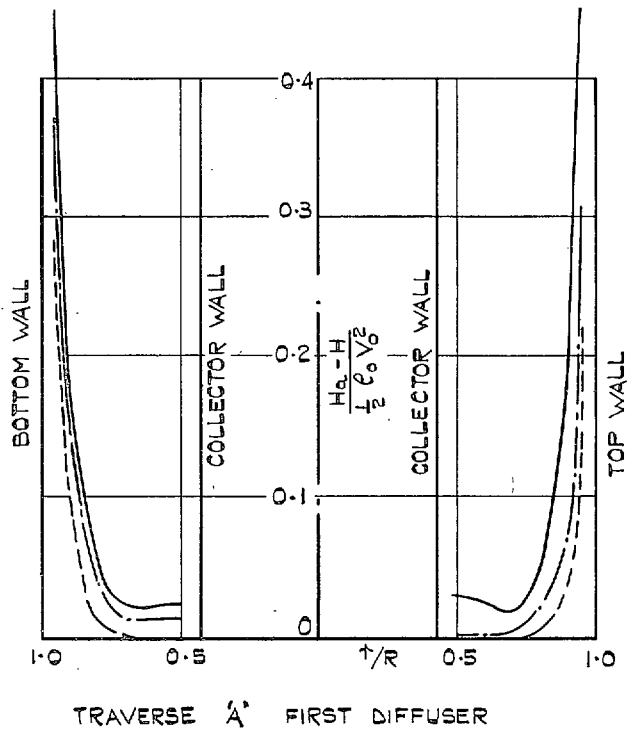
$M_o = 0.814$ ——— $\mu = 0.163$ 15·6 % COLLECTOR

$= 0.609$ —·—·— $= 0.160$ 15·6 % COLLECTOR

$= 0.199$ — — — $= 0.159$ 15·6 % COLLECTOR

TRAVERSE 'B' FIRST DIFFUSER
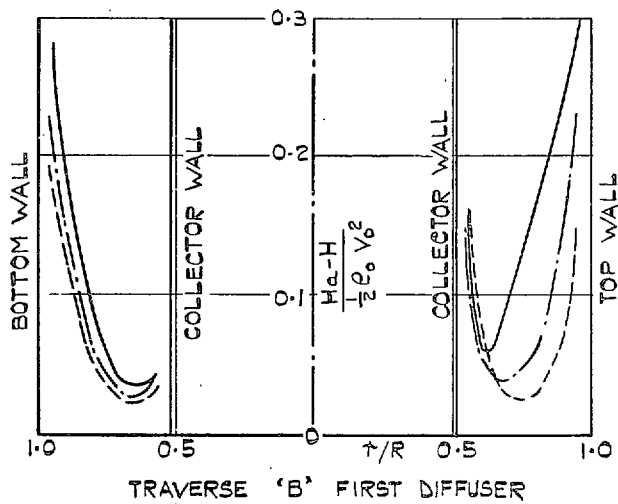
FIG. 13.   Total head traverses—first diffuser.
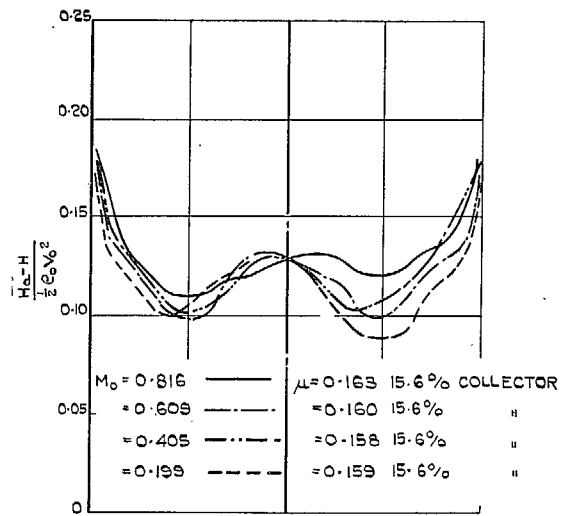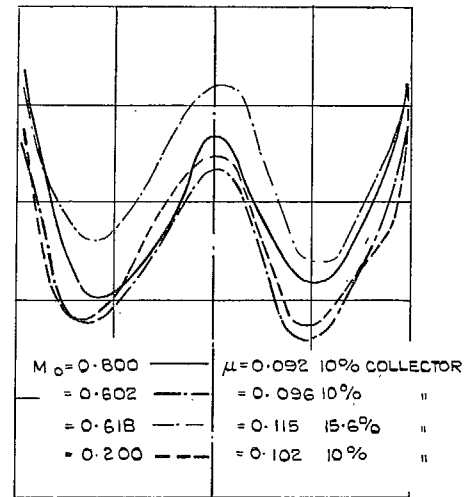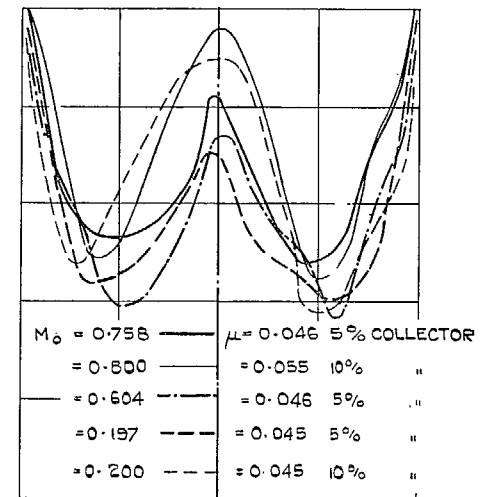
27
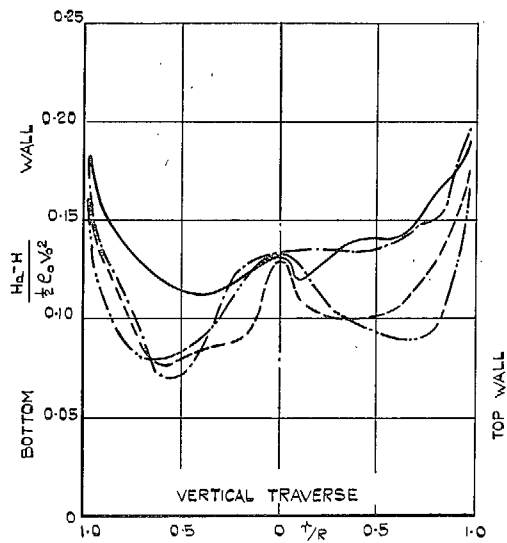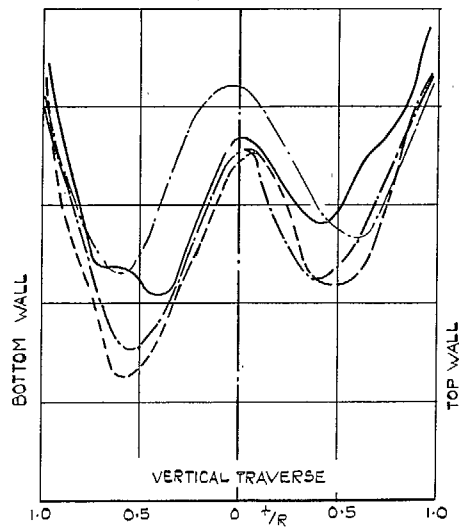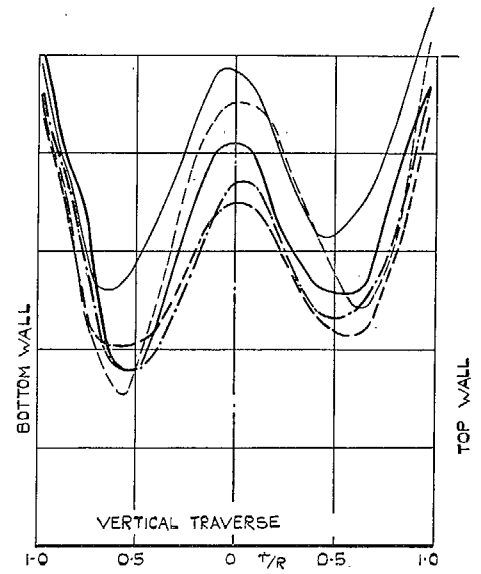
FIG. 14. Effect of Mach number and collector size on total head traverses at end of second diffuser.

28

$$M_0 = 0.604 \quad \underline{\hspace{2cm}} \quad \mu = 0.159, \ 15.6\% \ \text{COLLECTOR}$$
$$= 0.602 \quad \underline{\ \cdot \ \underline{\ \ } \ \cdot \ } \quad = 0.096, \ 10.0\% \quad \text{,,}$$
$$= 0.604 \quad \underline{\ -\ -\ -\ -\ } \quad = 0.045, \ 5.0\% \quad \text{,,}$$

$$\eta_{H_2} = \frac{Ha - H_2}{\frac{1}{2}\,\rho_0\,V_0{}^2}$$

TRAVERSE 'C'   TRAVERSE 'D'   TRAVERSE 'E'
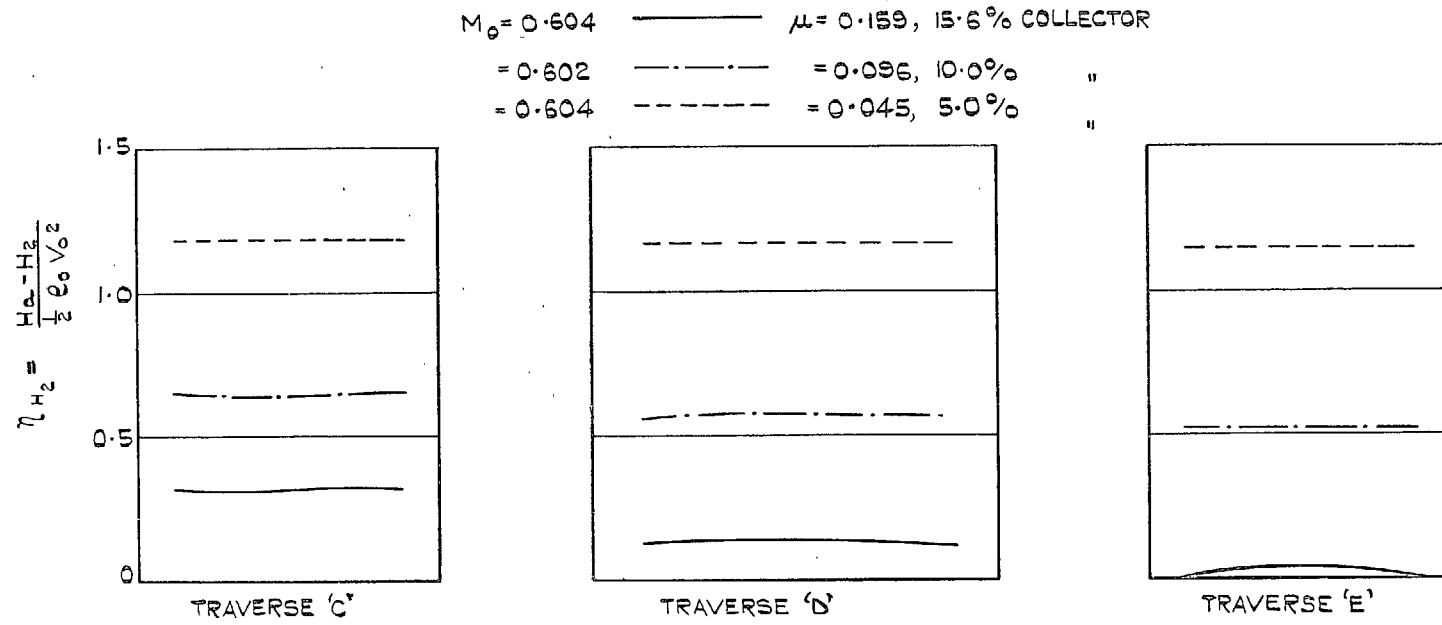
Fig. 15.   Effect of collector size, at geometric interchange ratio on typical total head traverses in interchange aerofoil ducts.
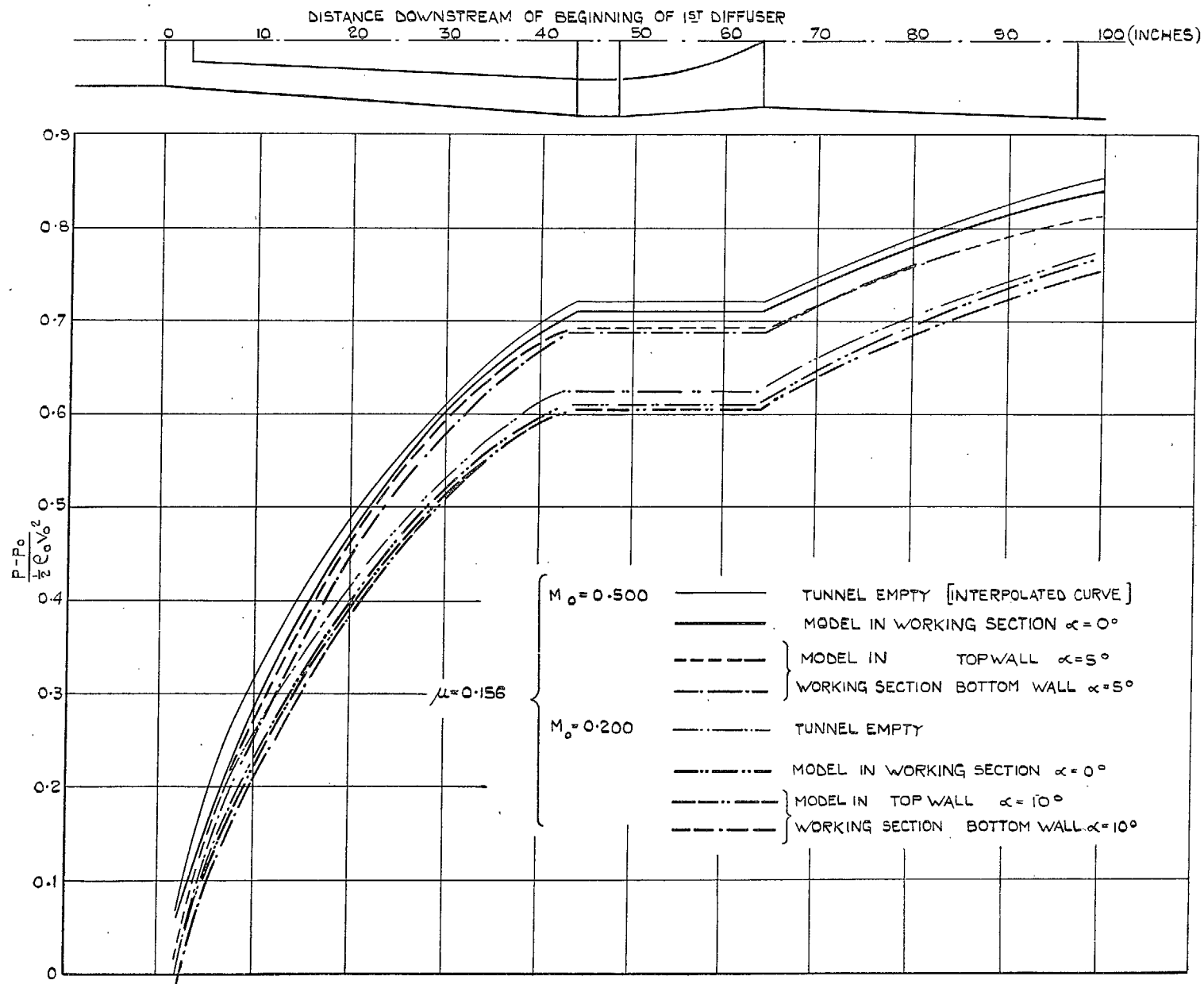
FIG. 16.   Effect of model in working-section on wall static pressure distribution in diffusers (15·6 per cent collector entry).
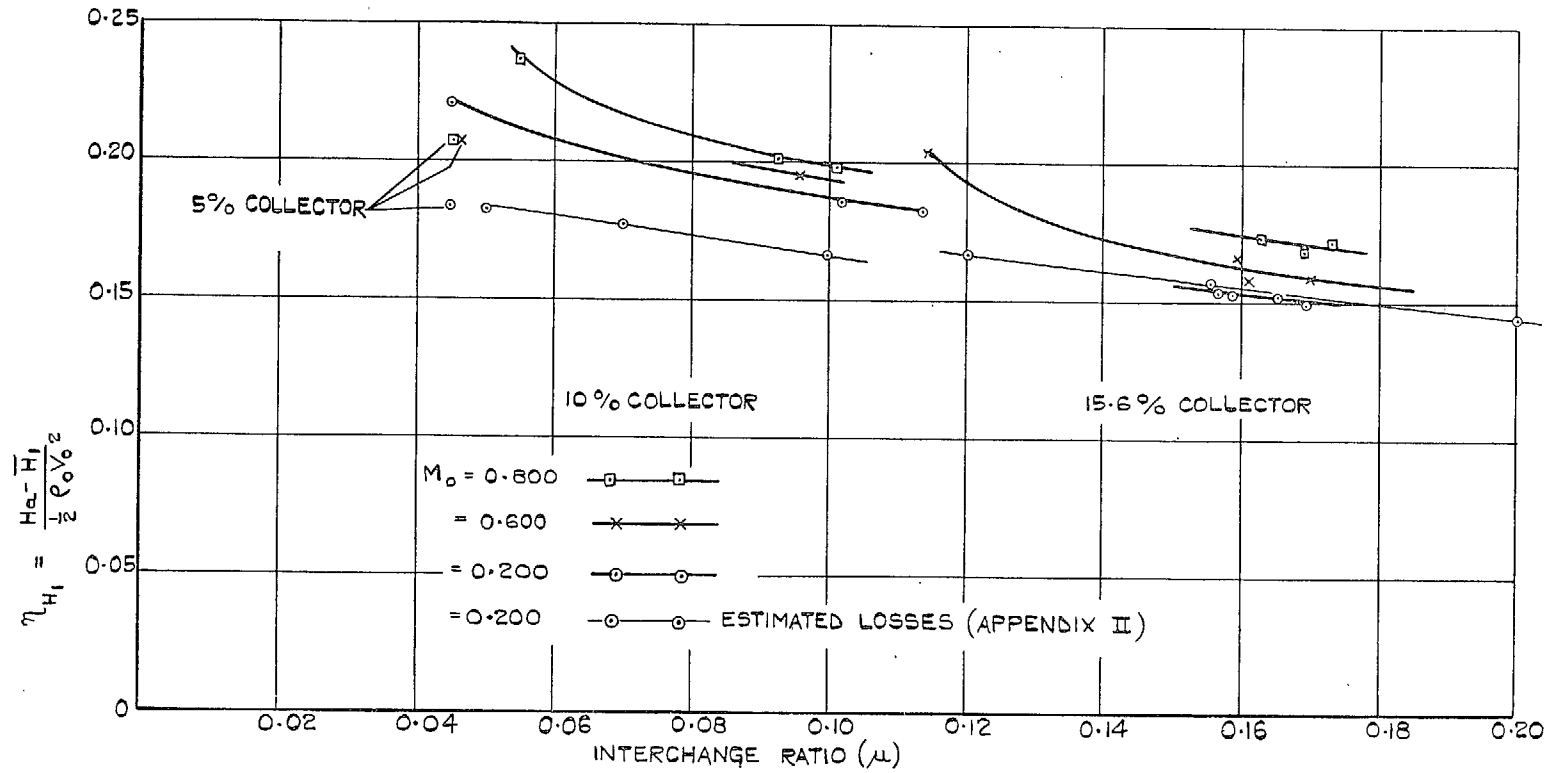
FIG. 17.   Variation of total head loss at end of second diffuser, with collector size, interchange ratio,
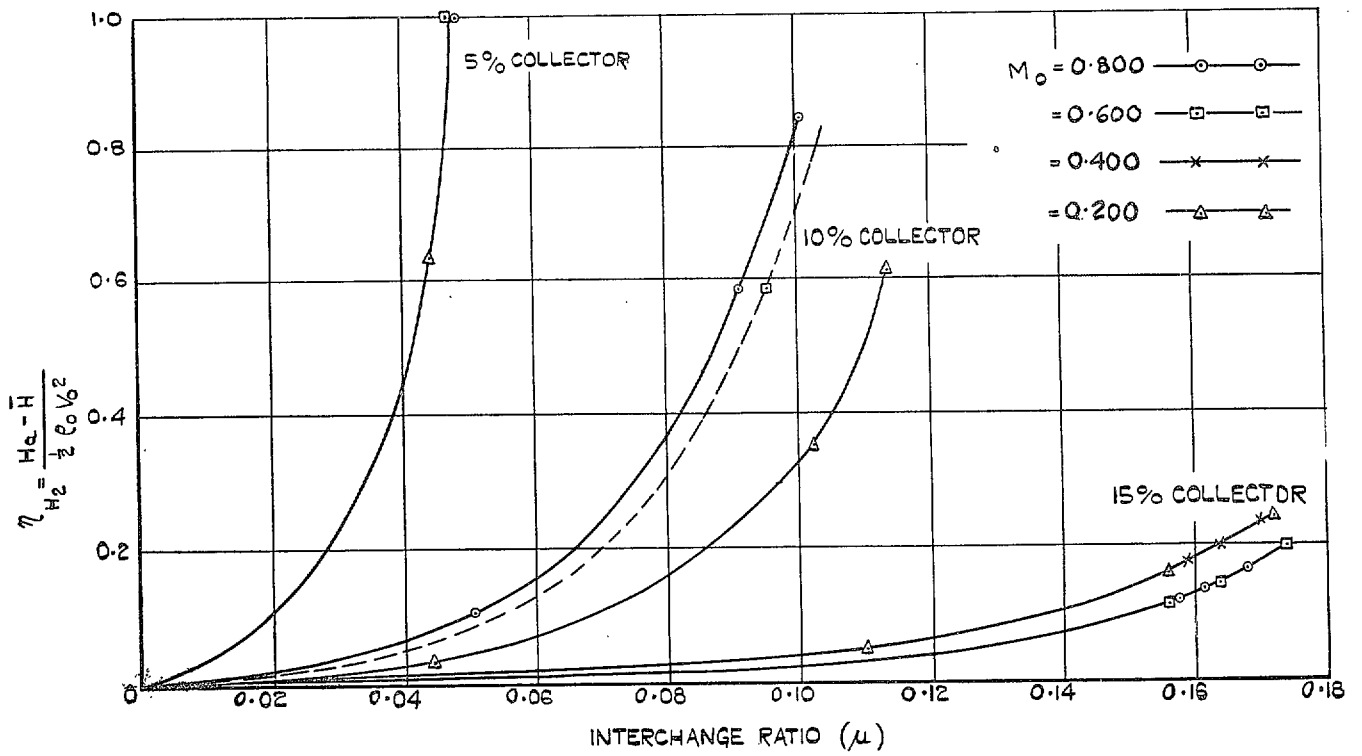and working-section Mach number.

FIG. 18. Variation of total head loss in interchange aerofoil ducts with collector size, interchange ratio and Mach number in working-section.
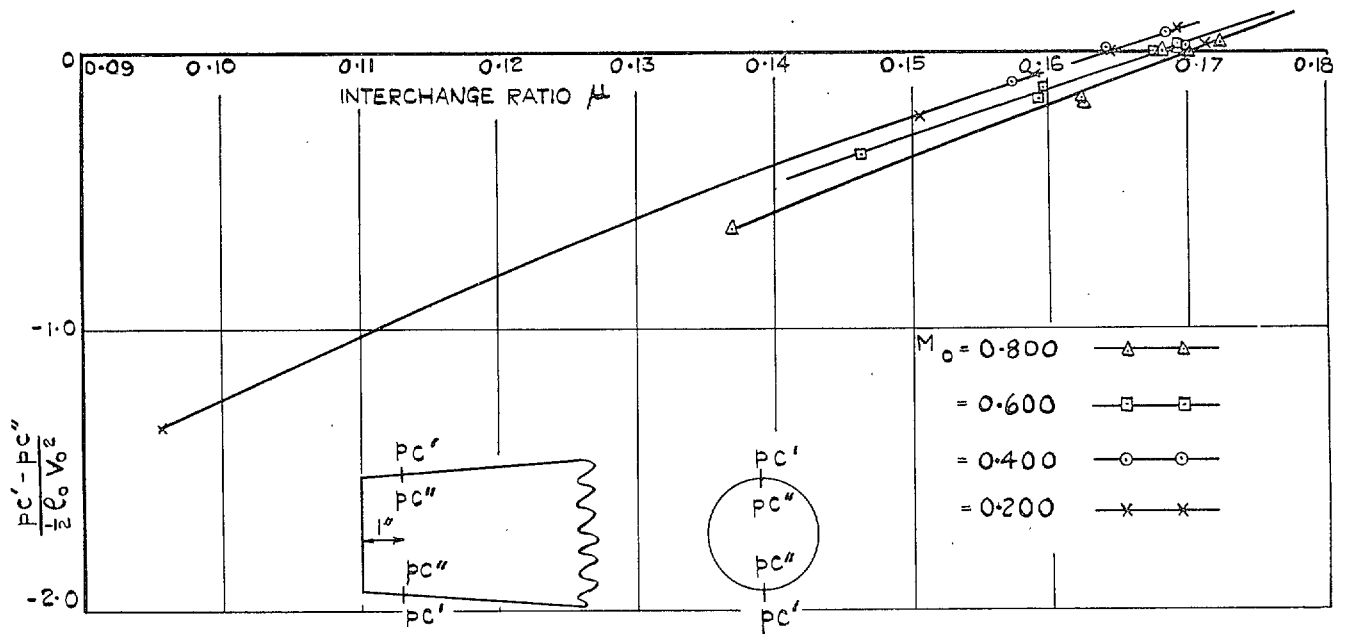

FIG. 19. Variation of pressure difference across collector entry with Mach number and interchange ratio (15·6 per cent collector).

Publications of the
Aeronautical Research Council

ANNUAL TECHNICAL REPORTS OF THE AERONAUTICAL RESEARCH COUNCIL
(BOUND VOLUMES)—

1936 Vol. I. Aerodynamics General, Performance, Airscrews, Flutter and Spinning.
40s. (40s. 9d.)
Vol. II. Stability and Control, Structures, Seaplanes, Engines, etc. 50s. (50s. 10d.)

1937 Vol. I. Aerodynamics General, Performance, Airscrews, Flutter and Spinning.
40s. (40s. 10d.)
Vol. II. Stability and Control, Structures, Seaplanes, Engines, etc. 60s. (61s.)

1938 Vol. I. Aerodynamics General, Performance, Airscrews. 50s. (51s.)
Vol. II. Stability and Control, Flutter, Structures, Seaplanes, Wind Tunnels,
Materials. 30s. (30s. 9d.)

1939 Vol. I. Aerodynamics General, Performance, Airscrews, Engines. 50s. (50s. 11d.)
Vol. II. Stability and Control, Flutter and Vibration, Instruments, Structures,
Seaplanes, etc. 63s. (64s. 2d.)

* 1940 Aero and Hydrodynamics, Aerofoils, Airscrews, Engines, Flutter, Icing, Stability
and Control, Structures, and a miscellaneous section. 50s. (51s.)

* 1941 Aero and Hydrodynamics, Aerofoils, Airscrews, Engines, Flutter, Stability and
Control, Structures. 63s. (64s. 2d.)

* 1942 Vol. I. Aero and Hydrodynamics, Aerofoils, Airscrews, Engines. 75s. (76s. 3d.)
Vol. II. Noise, Parachutes, Stability and Control, Structures, Vibration, Wind
Tunnels. 47s. 6d. (48s. 5d.)

* 1943 Vol. I. (In the press).   * Certain other reports proper to these volumes will
Vol. II. (In the press).   subsequently be included in a separate volume.

ANNUAL REPORTS OF THE AERONAUTICAL RESEARCH COUNCIL—

1933–34	1s. 6d. (1s. 8d.)	1937	2s. (2s. 2d.)
1934–35	1s. 6d. (1s. 8d.)	1938	1s. 6d. (1s. 8d.)
April, 1935 to Dec. 31, 1936. 4s. (4s. 4d.)		1939–48	3s. (3s. 2d.)

INDEX TO ALL REPORTS AND MEMORANDA PUBLISHED IN THE ANNUAL
TECHNICAL REPORTS, AND SEPARATELY—

April, 1950 . .. . . . R. & M. No. 2600. 2s. 6d. (2s. 7½d.)

AUTHOR INDEX TO ALL REPORTS AND MEMORANDA OF THE AERONAUTICAL
RESEARCH COUNCIL—

1909–1949 . .. . . . R. & M. No. 2570. 15s. (15s. 3d.)

INDEXES TO THE TECHNICAL REPORTS OF THE AERONAUTICAL RESEARCH
COUNCIL—

December 1, 1936 — June 30, 1939.	R. & M. No. 1850.	1s. 3d. (1s. 4½d.)
July 1, 1939 — June 30, 1945.	R. & M. No. 1950.	1s. (1s. 1½d.)
July 1, 1945 — June 30, 1946.	R. & M. No. 2050.	1s. (1s. 1½d.)
July 1, 1946 — December 31, 1946.	R. & M. No. 2150.	1s. 3d. (1s. 4½d.)
January 1, 1947 — June 30, 1947.	R. & M. No. 2250.	1s. 3d. (1s. 4½d.)
July, 1951.	R. & M. No. 2350.	1s. 9d. (1s. 10½d.)

Prices in brackets include postage.

Obtainable from

HER MAJESTY'S STATIONERY OFFICE

York House, Kingsway, London, W.C.2 ; 423 Oxford Street, London, W.1.
(Post Orders ; P.O. Box 569, London, S.E.1) ; 13a Castle Street, Edinburgh 2 ;
39 King Street, Manchester 2 ; 2 Edmund Street, Birmingham 3 ; 1 St.
Andrew's Crescent, Cardiff ; Tower Lane, Bristol 1 ; 80 Chichester Street,
Belfast OR THROUGH ANY BOOKSELLER.